A Wide Portray of Upconversion Nanoparticles: Surface Modification for Bio-applications

Monami Das Modak and Pradip Paik

Abstract Present days have spotted many innovations in research on upconverting nanoparticles (UCNPs) co-doped with lanthanoids (mostly Er^{3+}, Yb^{3+}/Tm^{3+},Yb^{3+}) through several synthetic approaches. A set of total 17 chemical elements (15 Lanthanides + Scandium + Yttrium) shows upconversion phenomena by exciting with NIR radiation (lower energy, longer wavelength) and finally results in visible light (higher energy, shorter wavelength) which makes it highly delightful for various applications. It is well known that for biological studies, fluorescence-imaging is an important phenomenon. Traditionally, as excitation radiation high energy lights are used which result in low energy emission by downconversion process. But, this phenomenon causes some difficulties like short tissue penetration depth, lower photo-chemical stability, lower sensitivity, cell death, DNA damage due to excitation with higher energy, whereas upconversion luminescence imaging gives better tissue penetration depth, good photochemical stability, improved sensitivity and very less probability of DNA damage and cell death as herein excitation is done with low energy photons and can be used in cancer therapy for destroying cancer cells with the emerging higher energy radiation. Herein, this reviews several current progresses with upconversion nanoparticles (UCNPs) in recent applications along with their different synthesis procedures, optical properties and growth of erection methods of different UCNPs applications have been highlighted based on their immobilization strategy.

Keywords Upconverting nanoparticles · Energy transfer · Emission · Immobilization · Biological applications

P. Paik (✉)
School of Biomedical Engineering, Indian Institute of Technology (BHU), Varanasi 221005, UP, India
e-mail: paik.bme@iitbhu.ac.in; ppse@uohyd.ac.in

M. Das Modak
School of Engineering Sciences and Technology, University of Hyderabad (UoH), Hyderabad 500046, TS, India

List of Abbreviations

UCNPs	Upconverting/upconversion nanoparticles
ESA	Excited state absorption
PA	Photon avalanche
ETU	Energy transfer upconversion
RE	Rare earth
TEM	Transmission electron microscopy
HRTEM	High resolution transmission electron microscopy
XRD	X-ray diffractometer
MRI	Magnetic resonance imaging
FRET	Fluorescent resonant energy transfer
PDT	Photodynamic therapy

1   Introduction

Upconverting nanoparticles (UCNPs) have already been established for prospective use as bio-labels and in biological analysis and bio-imaging which are the most promising technologies today. These promising and advanced technologies suggest that UCNPs could reconstruct the enduring technologies due to its ability to suspend as clear colloidal solutions (Boyer et al. 2007). Until now, the highest upconversion efficiencies have been remarked in $NaYF_4$ hexagonal phase co-doped with Er^{3+}/Yb^{3+} or Tm^{3+}/Yb^{3+} ion-pairs (Kramer et al. 2004; Suyver et al. 2005b).

Selection of host material is an important factor for achieving upconversion phenomenon properly. To achieve highest luminescence quantum yield and also less probability of occurring non-radiative relaxation, nowadays, fluoride is used in host materials such as REF_3 and $AREF_4$ (A = Alkali), and as a result, they help to increase refractive index and transparency, though Chlorides and Bromides can also enhance luminescence intensity but they are mostly sensitive to moisture, so difficult for imaging bio-molecules. Therefore, adding of fluoride in host materials is an increasing phenomenon today. Photon upconversion process is based on nonlinear optics, where the optical properties of material changes with the intensity of the incident exciting light. But are they noteworthy and adaptable enough to explain the difficulties of redirecting to a new technology, conventionally a lengthy and precious procedure? Could UCNPs become the upcoming wild materials reconstructing some of the contemporaneously used technologies and leading to the advanced research? Is it flexible as many as required to transmute many features in our life? By reviewing different proposed synthetic procedures allowing their several applications in different fields, those questions will be answered. Though there are several synthetic routes for preparing UCNP nanocrystals, among which hydrothermal synthesis has a lot of favourable advantages compared to the low reaction temp process (<250 °C); and it resulted in uniform distribution of size, shape and

morphology. The procedure and the experimental set-up used in these methods are easy to handle and very simple. In such case, basically three conditions are responsible to convert alpha (α-NaYF$_4$) phase to beta (β-NaYF$_4$) phase; they are high hydrothermal temperature, long hydrothermal time and high fluoride to lanthanide molar ratio (Suyver et al. 2005b).

So, initially, the observed properties in UCNPs will be discussed.

By Raman spectroscopy, it has been confirmed that the dominant phonon modes in undopped NaYF$_4$ lie in the range 300–400 cm^{-1}. These low energy phonon modes describe the remarkable upconversion efficiency (Zhao et al. 2008). By the implementation of the plasmonic effects, it is possible to enhance upconversion fluorescence which has been already done by directed nano-assembly of NaYF$_4$: Yb^{3+}/Er^{3+} nanocrystals with gold nanospheres (Suyver et al. 2006). From literature, it has been observed that, crystallographic size, crystallographic phase (Schietinger et al. 2010) and optical emission properties (Feng et al. 2006; Heer et al. 2004; Sivakumar et al. 2005; Ehlert et al. 2008) of such resultant nanocrytals can be controlled simultaneously by influencing them with dopant ions. By controlling concentration of trivalent lanthanide dopant ions, it is quite possible to tune size (down to 10 nm), shape (cubic to hexagonal) and upconversion (Wang and Liu 2008; Auzel 2004; Suyver et al. 2005a) emission colour (green–blue) of NaYF$_4$ nanocrystals. There are two factors of dopant ions, their size and dipole polarizability, that can change the crystal size and shape of resultant nanocrystals. UCNPs can offer high photochemical stability, sharp emission bandwidths and large anti-stokes shift (Wang and Liu 2009). There are four experimental variables which are solvent in nature, reaction time and temperature and metal precursor concentration that inflict stiff sway over crystallization of resultant particles with completely explained crystal phase and size. Hexagonal UCNPs phase structure is always preferable compared to cubic structure in various applications. There is a huge difference (almost by a factor 7.5) (Wang et al. 2010a, b) in fluorescence intensity between its cubic and hexagonal phase—nanoparticles. Inspite of these drawbacks, in cubic-phase, sometimes, we prefer cubic phases in as-synthesized UCNPs depending on their particular sizes, shapes, crystallinity, fluorescence properties and easy dispersion in non-polar solvent.

Generally, it has been noticed that the structure of NaREF$_4$ system for both cubic and hexagonal phase differs on the basis of F$^-$ cubes and ions present in them. In cubic structure, cations and vacancies sustain with uniform numbers of F$^-$ cubes whereas for hexagonal structure, F$^-$ ions are seated in an ordered array, to fit the structural change, electron cloud deformation of cations is crucial (Fig. 1). Basically, one ordered way is maintained for lanthanides. As lanthanide series starts from lanthanum (La), finishes with Lutetium (Lu) (Lanthanide series-La, Ce, Pr, Nd, Pm, Sm, Eu, Gd, Tb, Dy, Ho, Er, Tm, Yb, Lu), now if we move towards higher atomic no. and lower atomic mass, i.e. from La to Lu, weight will decrease and ionic radii will increase, dipole polarizibility increases, tendency towards e-distortion cloud increases which is the appreciative condition for hexagonal phase. So formation of hexagonal phases in lanthanides having higher atomic number will be more than that of having lower atomic number. Size of Y^{3+} ion is ($r = 1.159$ A$°$) in NaYF$_4$ host lattice. More hexagonal phases will be produced for doped lanthanide ions having
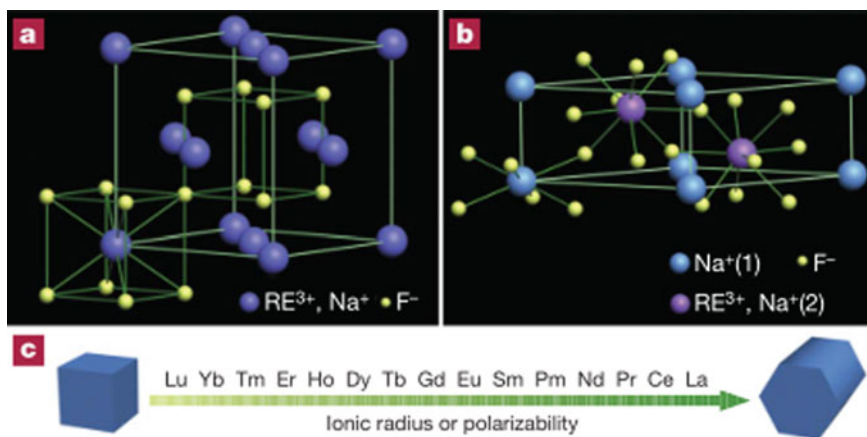
Fig. 1 Schematic of phase transformation in Na [Rare Earth (RE)] F_4 while doped with lanthanides, **a** cubic phase, cations and vacancies sustain with equal numbers of F^- cubes, **b** hexagonal phase, two types of cation sites sustain with an ordered F^- ion-array (Na^+, RE^{3+}/Na^+), **c** shows the fashion of cubic-to-hexagonal phase transition as a function of ionic radius/polarizability of elements present in lanthanoid-series. Reproduced with permission (Wang et al. 2010a, b). *Copyright* Nature publication

larger size (i.e. for Gd^{3+} ion $r = 1.193$ A°)than the size in Y^{3+} in host lattice and finally the growth of unit cell volume occurs due to the presence of larger-sized lanthanide dopant ions (Wang and Liu 2009).

2 Challenges in Production

There are several applications of UCNPs having different shapes, sizes and structures which can be significantly controlled by their development with a number of designed synthesis procedures and their dispersions in various media. Now, depending on the notable properties and the quality of UCNP (either in dried or in colloidal form) in as-synthesized materials, they can be used in different potential applications such as in silicon-based solar cell as spectral converters (Yi and Chow 2006; Xie and Liu 2012), in optical imaging and MRI as a multimodal contrast agent (Zou et al. 2012), in FRET bio-sensors (Park et al. 2009); as colour display (Wang et al. 2005a, b), versatile bio-probes in biomimetic surface—engineering (Kim et al., 2009), nanoprobes for sensing and imaging of pH, cells and small animals(Li et al., 2012), nano-transducers for killing diseased cells in deep tissues (Chatterjee et al., 2008), the most viable luminescent bio-labels in bio-conjugation and bio-imaging (Chatterjee and Yong, 2008). Therefore, the production of those UCNPs with required sizes, shapes and structures is very crucial for different applications. During their preparation, all the reaction parameters are being controlled in a precise manner due to the high sensitivity

of the products through their formation periods. And thus the production of UCNPs is challenging.

If we go through the literature reviews, we will find that mostly several optical properties became prominent for their applications. This is the main property for which they are being broadly used in nanotransducers (Chatterjee et al. 2008; Mader et al. 2010), broad brands (Yi and Chow 2006; Xie and Liu 2012), Imaging contrast agent (Zou et al. 2012), multimodal imaging (Idris et al. 2012; Cheng et al. 2011a, b), superresolution-nanoscopy (Xu et al. 2011; Liu et al. 2017), imaging probes (Zhan et al. 2017) and so on. Therefore, review has been focused briefly on optical properties with possible photonic processes for UCNPs.

3 Optical Properties

Lanthanoids exist in lanthanide series and there are a total of 15 lanthanoids. Though transition metals (Scandium, Yttrium), where atoms have partially filling 'd' sub-shell and elements in actinide series can exhibit upconversion phenomena, but specially RE elements having combination of 15 lanthanoids + Scandium + Yttrium, a set of total 17 chemical elements show upconversion phenomena very strongly, i.e. by exciting that lanthanide-doped nanocrystals with NIR radiation. In the upconversion process, we can get visible light with the emission of higher energy photons. Thus, upconversion process converts low energy, long wavelength NIR radiation to high energy, short wavelength visible light. The optical properties of upconversion nanoparticles arise due to conversion of near infrared radiation (NIR) into visible spectral range which is a very efficient phenomenon in rare earth-based materials. The nanocrystals based on rare earth ions showed strong upconversion emission with a continuous excitation wavelength at 973 nm (Suyver et al. 2006). Therefore, they have a great potential in applications of solid-state laser materials as well as several lighting, panel and colour display technologies (Yang et al. 2014; Scheps 1996). It is well known to us that $NaYF_4$ nanocrystals co-doped with Yb^{3+} and Er^{3+}/Tm^{3+} are the most promising upconverting nanomaterial today as these nanocrystals are sensitized by Yb^{3+} (sensitizer) and multicolour wavelength range can be distinguished from Er^{3+} or Tm^{3+} (activator) dopant ions.

Experimentally and theoretically it has been already proven that most of the lanthanide ions exhibit visible light under excitation with NIR radiation but sharp luminescence imaging can be observed by upconversion process under 980 nm excitation if some of them such as Er^{+3}, Tm^{+3} are co-doped with the host lattice like $NaYF_4$, hence the productive forms are written as $NaYF_4$: Yb^{3+}; $Er^{3+}/NaYF_4$: Yb^{3+}; Tm^{3+}.

Some important luminescence properties can be observed with using such UCNPs such as narrow band width with shorter wavelength compared to the excitation wavelength, i.e. anti-stokes-type emission (Wang and Liu 2008) and long-time emission. To get upconversion phenomenon properly, choosing of host material is an important factor. To achieve highest luminescence's quantum yield, and also less probability of

occurring non-radiative relaxation nowadays, fluoride is used in host materials such as REF_3 and $AREF_4$ (A = Alkali), as a result they help to increase refractive index and transparency though chlorides/bromides can also enhance luminescence intensity. However, they are very sensitive to moisture and possess difficulty for imaging of bio-molecules and cells. To overcome this limitation, fluoride molecules are added in the system. The main difference between fluorescent and luminescent materials is their different characteristics. Fluorescent materials absorb high energy photons with the emission of visible light and low energy photons, which results in auto fluorescence, wide emission bands and limited sensitivity. To overcome these difficulties, upconverting luminescent nanoparticles with high quality developed promptly. Trivalent rare earth (RE) ion (Ho^{3+}, Er^{3+}, Tm^{3+}) follows upconversion process fairly (Downing et al. 2006). By incorporating a few energy transfer related mechanisms, we will try to understand the photon-generation mechanism in UCNPs.

There are some basic mechanisms which results in highest population in excited state and after that when they come in the ground state, emit high energy photons. Multiphoton absorption occurs by the excited state absorption mechanism (ESA) (Downing et al. 2006) (Fig. 2) which further involves multistep excitation by the same ion and finally highest population occurs at the excited state. This process is also known as phonon-assisted electronic transitions (Yang et al. 2014; Downing et al. 2006).

Suppose, energy of incident photons has flux ϕ (Say) is resonant with the energy difference ($E_1 - E_0$), then some of the photons are absorbed from the ground state by the particular ion. Similarly, while the energy of the incident photons having certain flux resonant with the energy difference ($E_2 - E_1$), then only incoming photons can be absorbed in the intermediate state by the same ion. Now, the population in the excited state becomes high and consequently the ion reaches to its high excited state, but this phase is not stable from this excited state and finally, upconversion luminescence occurs by radiating photons. We have considered this process for a single ion so we can assume that it is independent on ion-concentration. According
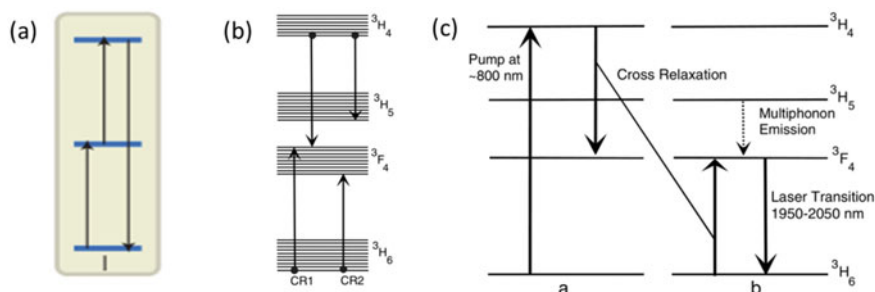

Fig. 2 a Excited state absorption mechanism (ESA). Reproduced with permission (Wang et al. 2011). Copyright: Nature Materials publication, **b** detailed energy-level diagram of the four multiplets of the Tm^{3+} ion. Reproduced with permission (Jackson 2004). Copyright: Optics Communications publication, **c** Two energy transfer upconversion processes (ETUs). Reproduced with permission (Jackson 2004). *Copyright* Optics Communications publication

to literature, anti-stokes fluorescence is proportional to the incident photon flux such that, for above-mentioned case, fluorescence is directly proportional to the square of the incident photon flux. ESA process is quite relative with the laser pumping process. As it avoids transfer losses, so it is assumed to be a suitable pumping process for upconversion single-doped mechanism. In ESA case, finally, we can conclude that by absorbing atleast two photons having sufficient energy, a single ion can reach its emitting level from which it undergoes luminescence.

Unlike ESA, (Fig. 2) where energy transfer upconversion process ETU is a pump power independent process and it involves two ions system—one is sensitizer ion and another one is activator ion. Sensitizer ion (S) can transfer its energy to activator ion (A) as they are placed much closer to each other. On excitation with suitable light, 'A' goes from its ground state to excited state and it is only possible if excited energies of two ions are equal or nearly equal to each other. After reaching the excited state, S ion can transfer its energy to the nearly placed A-ion whose excited state energy is equal. Here, it is to be notified that before emitting photons by S-ion, A goes from ground state to the excited state. Cross relaxation (CR) and energy transfer profess are very important in upconversion phenomenon. Cross Relaxation occurs due to overlapping of the spectra (Joubert 1999). For example, in Silica between $3H_4 > 3F_4$ Fluorescence spectra, there is a strong overlapping between them. Previously, it has already examined for Tm^{3+}-doped silica fibre lasers. The cross-relaxation mechanism with its energy-level diagram (Joubert 1999) of the four multiplets $3H_6$, $3F_4$, $3H_5$, $3H_4$ is shown in Fig. 2b.

Several spectral properties of RE-doped UCNPs have huge scope in biomedical imaging and therapeutics (Jackson 2004; van de Rijke et al. 2001; Hampl et al. 2001). Other exciting optical properties in the same material can be aroused by tuning their spectral properties in a proper way. Surface plasmon resonance caused by the interaction of metal with the incident light assists for different interesting optical events like radiative and non-radiative properties of nanocrystals (Lim et al. 2006; Zhang et al. 2010; Eustis and Sayed Eustis and El-Sayed 2006). In literature, the Raman spectroscopy with dominant phonon modes ($300-400$ cm^{-1}) of such RE-based materials has been already demonstrated (Zhao et al. 2008).

4 Different Synthetic Strategies for the Production of Upconversion Nanoparticles

Earlier, we have already discussed, choosing of host materials is a very important factor to UCNPs as they determine their quality. Now, to get better quality (such as better luminescence efficiency, chemical stability, low phonon energies giving low probability of non-radiative decay), synthesizing UCNPs in a proper way is very crucial key. Synthetic routes for upconversion nanoparticles are based on mainly three strategies: thermal decomposition, Hydrothermal or solvo-thermal synthesis,

ionic—liquid based or ionothermal synthesis. Hence, we will discuss a variety of synthetic routes based on those three basic strategies.

4.1   Thermal Decomposition

To control the shapes and sizes of nanocrystals, thermal decomposition is one of the most familiar and popular method. As reagents,organic precursors (e.g. trifluoroacetate precursor), surfactants(oleic acid, oleylamine) and organic solvents are used. By product what we get is nuclei form of our desired nanocrystals which then goes under growth mechanism. There after dissolution and aggregation take place. Thermal decomposition follows overall four stages—Nucleation, Growth, Dissolution and Aggregation.

Most of the RE fluorides are synthesized by this route. Some examples of such prepared UCNPs are $NaYF_4$: Yb, Er; $NaYF_4$: Yb, Tm; $NaGdF_4$: Yb, Er; $NaGdF_4$: Yb, Tm; $NaLuF_4$: Yb, Er; NaLuF4: Yb, Tm, CaF_2, etc.

Drawbacks of thermal decomposition: Though thermal decomposition gives well shaped and sized monodispersed particles (Barnes et al. 2003), still it holds some disadvantages like

(a) Requires temperature in the range of 250–330 °C, which is quite high. During maintenance, such high temperature sometimes may cause burning, particle-aggregation and particle-enlarging.
(b) Surfactants having long hydrocarbon chains and polar capping groups associated with organic precursors during synthesis can yield difficulties for biological applications especially while we are using them for stabilizing nanomaterials.
(c) Requires high-boiling organic solvents to dissolve organic precursors.
(d) To overcome the difficulty of using surfactants, sometimes, we need surface modification/engineered modified surface which can be cost-effective.
(e) Ideal condition of this experimental set-up is always being used in an complete oxygen-free inert gas condition which is difficult to handle during synthesis, even a very small amount of oxygen during synthesis may damage and form an unsuccessful product.

Inspite of having the above-mentioned drawbacks in thermal decomposition procedure, this process has already been investigated with the production of Alpha-$NaYF_4$: 20%Yb, 2%Er (cubic-phase) and Beta-$NaYF_4$: 20%Yb, 2%Er (hexagonal phase) nanocrystals in a large-scale area where successful synthesis of co-doped $NaYF_4$ nanocrystals has been built-up with thermal decomposition procedures. The final shapes, sizes and structures of UCNPs can be changed by modifying or varying the reaction time, reaction temperature, reagent concentration and the resulted modified nanocrystals can be characterized using transmission electron microscopy(TEM), high-resolution transmission electron microscopy (HRTEM), field emission scanning electron microscopy (FESEM) and X-ray diffraction (XRD) patterns.

By introducing two synthetic procedures (Barnes et al. 2003; Boyer et al. 2006), collecting from different literature, hereby, I will describe the thermal decomposition with their required precursors, reaction temperature and reaction time. At a recent time, Gudel et al. (Boyer et al. 2007; Kramer et al. 2004; Zhao et al. 2008; Feng et al. 2006) spotted micrometre-sized hexagonal phases of $NaYF_4$: Yb^{3+}, Er^{3+}/Tm^{3+} crystals which are enable to show highest upconversion efficiencies. It is familiar to us that metal trifluoroacetates thermally decompose providing their corresponding metal fluorides, fluorinated and oxyfluorinated carbon species (Russel 1993; Rillings and Roberts 1974), whereas lanthanide trifluoroacetate precursors can be formulated from their corresponding lanthanide oxides and trifluoroacetic acid (Russel 1993).

TEM images of the colloidal UCNPs ($NaYF_4$ co-doped with Er^{3+}/Yb^{3+} and Tm^{3+}/Yb^{3+}) formed via thermal decomposition procedure are shown in Fig. 3 with two histograms of particle size distribution (histogram result between Number of Particles and Particle Diameter (nm) for Upconverting Nanocrystals).
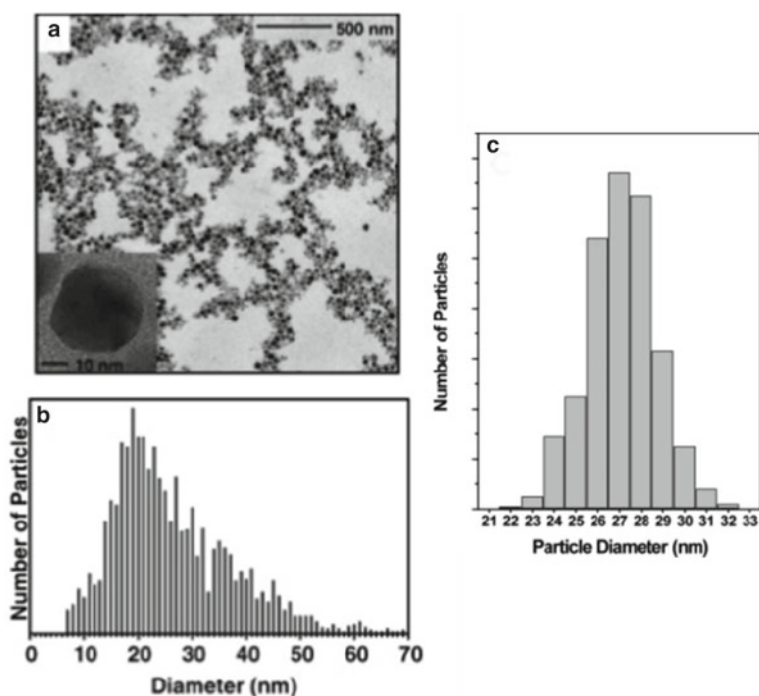

Fig. 3 **a** TEM image, **b** histogram for obtained particle sizes with ~1400 nanocrystals. Reproduced with permission (Boyer et al. 2006). Copy right: Journal of American Chemical Society publication, **c** histogram of obtained particle sizes with ∼500 nanocrystals. Reprinted with permission (Boyer et al. 2007). *Copyright* Nano Letters publication

4.2   Hydrothermal or Solvothermal Synthesis

A convenient synthesis process for producing UCNPs with overcoming some of the difficulties associated with thermal decomposition process is termed as hydrothermal or solvothermal synthesis procedure. The advantages of this process over thermal decomposition are given by following.

(a) Temperature required is relatively low (160–220°) compared to that in thermal decomposition.
(b) Oxygen-free inert gas condition is not required and that's why it is easy to handle.
(c) Organic compounds are not required as this process involves water solution phenomena.
(d) Various nanocrystals with hexagonal and octodecahedral shapes can be formed or synthesized applying this method. By adding several fluoride sources and organic additives (e.g. trisodium citrate), we can get desired shapes and sizes with different morphologies and architectures.
(e) Synthesis through hydrothermal/solvothermal synthesis has been given in various literatures (Wang and Li 2007; Sun et al. 2006; Li et al. 2007; Mi et al. 2011).

Advantages of hydrothermal synthesis over others and morphological effect of resultant particles on hyderothermal time, tempereatures and on other parameters: Compared with the other synthetic routes, hydrothermal synthetic procedure is superior following some advantages like,

(a) At relatively lower temperature (<250 °C), synthesis can easily happen and during synthesis by changing concentration of precursors, nature of solvent reaction time and other experimental parameters size, structure and morphology of the resulting products can easily be modified.
(b) Experimentally, it has been observed that the purity of the resulting particles become significant in case of hydrothermal synthesis.
(c) The synthetic process and the required equipment used in such experiment are simpler and easier to handle.
(d) Sometimes, organic additives (EDTA, citrate) are used during synthesis to get small and uniform particles. The resultant size of particles differs with different organic additives due to their different chelating agent and molecular structure providing morphological product. The main reason behind that difference is the influence of chelator on the growth of particles (Yi et al. 2004). As for example, size of the particles synthesized with citrate is much less than that synthesized with EDTA.

There are generally four factors which substantially affect the size, structure and morphology of the resulting nanocrystals. They are described as follows:

(a) *Effect of fluoride–lanthanide molar ratio*: The amount of NaF content is counted in NaF: Ln molar ratio to investigate its effect on size, structure and morphology

Table 1 Different crystallization, shape and surface pattern with different amount of NaF:Ln ratio

NaF:Ln molar ratio	Crystallization	Shape	Surface pattern
4	Low crystallization of the sample providing more likely fcc (Suyver et al. 2005b; Wei et al. 2006)	Spherical	Coarse surface
8	Improved crystallization	More regular shape	More smoother surface
12	Further improved	Pure hexagonal-shaped sub-microplates	Further improved

of the resulting UCNPs. Larger the fluoride–lanthanide ratio provides the better crystallization, more regular and smoother surface, more hexagonal phases (i.e. influence the crystal structure as fcc or hexagonal) of the resulting nanocrystals. Now, the effect of NaF: Ln ratio on crystallization, shape and surface pattern of the synthesized Yb^{3+} and Er^{3+} co-doped $NaYF_4$ nanocrystals is shown in Table 1.

From Table 1, it is clear that the effect of NaF content on the crystal morphology plays an important role as the crystal phase is completely transformed into hexagonal phases at the NaF:Ln molar ratio of 12 or above.

(a) *Effect of citrate–lanthanide ratio*: In hydrothermal method, chelating agent has appreciable effect on size and aggregation of the particles. Therefore, by choosing proper chelating agent, it is quite possible to produce small-sized and dispersible nanoparticles (Suyver et al. 2005b; Sun et al. 2007). Therefore, citrate: Ln ratio plays an important role in forming different morphologies (Table 2).

In conclusion, the formation of cubic crystal structure is possible with citrate–lanthanide and ratio is greater than unity (citrate: lanthanide > 1) and with citrate–lanthanide ratio is less than unity there exist mixed phases (cubic and hexagonal) in resulting crystal structure (citrate: lanthanide < 1).

Table 2 Molar ratio of chelator: Lanthanide affecting the morphologies of $NaYF_4$: Yb^{3+}, Er^{3+} nanocrystals

Molar ratio of citrate–lanthanide	Morphology of the resulting particles
0:1 (i.e. without citrate)	Formulation of resulting nanoparticles as mixtures of nanorods as well as spherical nanoparticles
0.5	A mixture of cubic nanoparticles and hexagonal submicroplates
1.0 and 1.5	Development of pure nanoparticles having size distribution in the range between 30–50 nm (with the restriction of the crystal growth)

(a) *Effect of Hydrothermal temperature*: Generally, the hydrothermal required temperature in the range between 160 and 200 °C to eventuate phase transformation. At higher hydrothermal temperature, cubic to hexagonal phase transformation is possible owing to generation of energy. Lower hydrothermal temperature approves smaller-sized nanoparticles having cubic phases, whereas higher hydrothermal temperature approves the formation of nanocrystals and sub-microplate mixture having hexagonal phase.

(b) *Effect of Hydrothermal time*: Hydrothermal time affects the crystallization and growth of the resulting nanocrystals. Long hydrothermal duration is favourable for the transformation of cubic phases into hexagonal phases. The hydrothermal time increases the rate of several processes during synthesis such as dissolution, re-nucleation and crystallization processes. In literature, it has been described that pure hexagonal phase—microplates (our required phase) of $NaYF_4$ nanocrystals have been found with hydrothermal time around 2 or 2.5 h (keeping citrate: lanthanide ratio = 1:1; and temperature at 180 °C) (Suyver et al. 2005b).

TEM images of the upconversion nanoparticles (YVO_4: Er^{3+}) synthesized with hydrothermal/solvo-thermal treatment are shown in Fig. 4.

4.3 *Ionic-Liquid Based or Ionothermal Synthesis*

Although pure hexagonal phase (which can yield better upconversion than the cubic one) can be obtained by this method, however, it is comparatively less popular than the previous two methods because it holds certain limitations while synthesizing nanocrystals, e.g.

(a) Nanocrystals used must be non-flammable
(b) Does not require any organic solvent.
(c) Produced particles become broader in size with lower quality (less uniformity, less monodispersity, less chemical stability) than the other two processes.
(d) Various shapes and sizes cannot be found by using ionothermal synthesis, only water-soluble hexagonal phase formation is possible.

Due to these above-mentioned limitations, it can be used only for preparing a few selective nanocrystals. Inspite of having such limitations, few advantages are also present such as.

(a) Reaction occurs within a very short period of time.
(b) Requires low temperature range and vapour pressure which are easy to control.

Earlier, synthesis procedures for the production of β-phase $NaYF_4$ nanomaterials were developed (Wang et al. 2010a, b, 2011; Wang and Li 2007; Wei et al. 2006; Yi and Chow 2007; Zeng et al. 2005; Mai et al. 2006) with the formation of particles of size ~15 nm where most of the synthesis procedures required in high-boiling solvents or in their mixtures (e.g. oleic acid, oleylamine, 1-octadecene or their
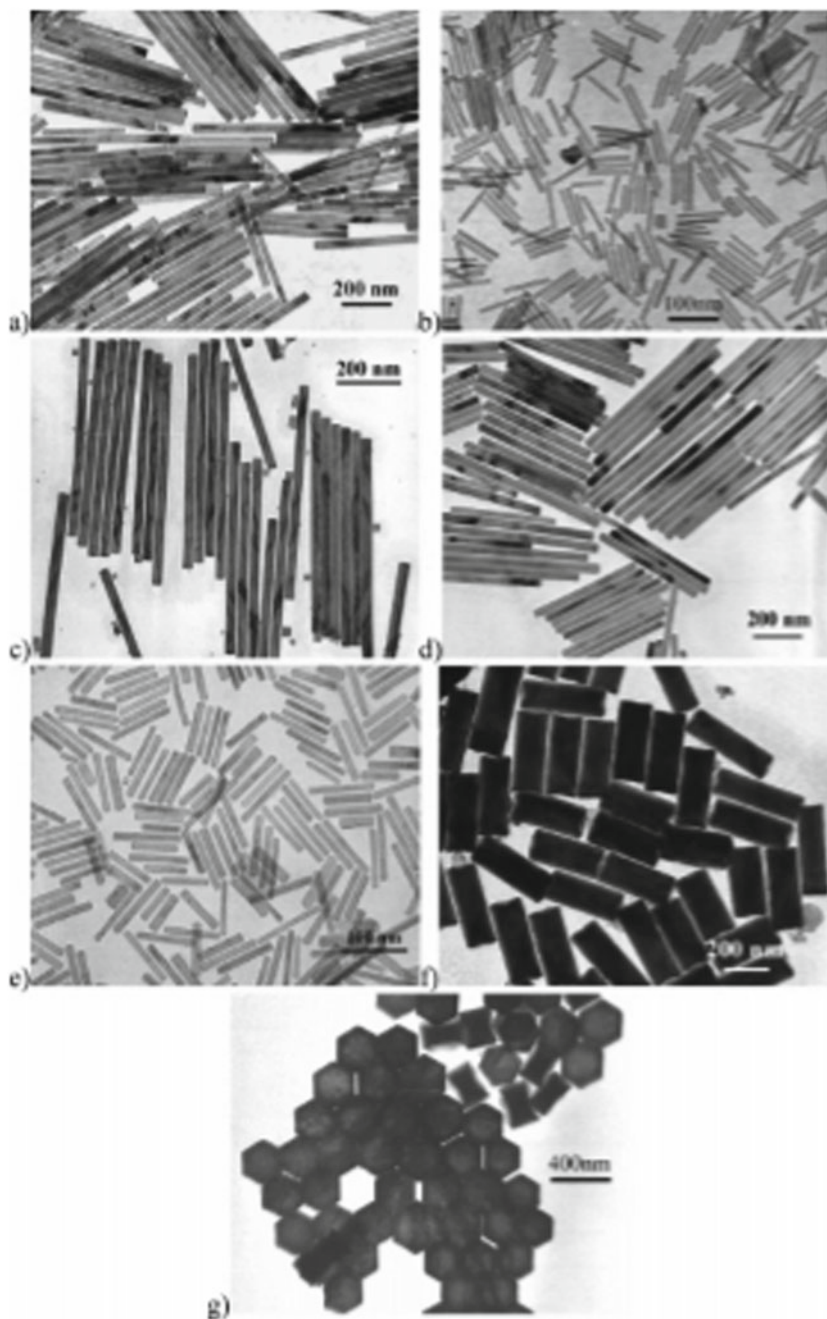
Fig. 4 TEM images of the resulted nanocrystals after solvo-thermal treatment. Reproduced with permission (Wang and Li 2007). *Copyright* Chemistry of Materials publication

solvent mixtures) owing to co-thermolysis of rare earth trifluoroacetates and sodium trifluoroacetate (Boyer et al. 2006). But these resulting luminescent nanomaterials seem to be difficult while using in bio-probes due to their sizes, not only that but also from literatures, it is revealed that they require a very high reaction temperature and yield rather very low compared to the other methods. Therefore, production of smaller size of such nanoparticles with high yield is a demanding matter in Bio-probe imaging. Chow et al. group synthesized 10-nm-sized hexagonal phase UCN nanocrystals in oleylamine at temperature above 300 °C having very narrow size distribution and introduced multiple precursors, e.g.—CF_3COONa, $(CF_3COO)_3Y$, $(CF_3COO)_3Yb$, $(CF_3COO)Er/(CF_3COO)_3Tm$, etc. (Wang et al. 2010a, b; Schafer et al. 2009). An average size of 7 nm of Yb^{3+}, Er^{3+} co-doped $NaYF_4$ nanocrystals were being synthesized at elevated temperature by Schafer group (Schafer et al. 2009).

For synthesizing, UCNPs precursor's properties also play a significant role in controlling size, shape and morphology. $NaYF_4$ nanocrystals co-doped with Er^{3+} and Yb^{3+} can be synthesized in the presence of precursors like-$Y_2(CO_3)_3$, $Yb_2(CO_3)_3$, $Er_2(CO_3)_3$, Na_2CO_3 and NH_4F as they can produce nanocrystals even at room temperature or at very low temperature having hexagonal phase (β-phase) giving better luminescence and high yield. This is one of the noteworthy advantages of these precursors providing a novel method of synthesis procedures at nanoscale production. Such novel synthesis method is based on the reaction of metal carbonates with Ammonium fluoride and synthesized in organic solvents in the range of temperature 20–280 °C. After decomposing of metal precursors pure, nanosized $NaYF_4$ nanocrystals co-doped with Er^{3+} and Yb^{3+} were formed having high yielded particles which are well separated and they contribute to broad size distribution (particle size ~4–10 nm). Thus, the transparent solution of these resulted nanoparticles exhibited visible upconversion emission on 978 nm of wave excitation. After that novel synthesis all the diffraction peaks appeared by XRD assign to hexagonal phases and no cubic phases are assigned, that means here, as all the phases belong to hexagonal phase, so, luminescence efficiency which is our desirable property becomes high. Cubic phase of Er^{3+} and Yb^{3+} co-doped $NaYF_4$ nanocrystals can be produced at elevator temperature (250 °C). All these reactions were done in pure oleylamine which can be replaced with oleic acid–oleylamine mixtures to discontinue the cubic phases formed in reaction. With the above-mentioned precursors under optimized conditions, 7-nm-sized particles (estimated as an average particle size) were formed having 84% yields (Schafer et al. 2009). Er^{3+}, Yb^{3+} ions coupled in hexagonal phase $NaYF_4$ matrix provides highest up conversion efficiency (Kramer et al. 2004; Yi and Chow 2007). Proper heat treatment is an important factor to increase the luminescence efficiency.

Thus, solid-state-reaction procedure is another way to form nanoscale hexagonal $NaYF_4$ powder with releasing ammonia at room temperature grinding dry powders (such as Na_2CO_3, NH_4F, and RE carbonates powders). But, owing to the presence of higher percentage of α-phases and other phases/impurities rather that β-phases in the as-synthesized sample, this procedure carries less importance compared to the

others mentioned above. Not only that but also it requires high reaction temperature (~300 °C or above) during synthesizing upconversion nanocrystals.

Ionothermal synthesis is the procedure where ionic liquids are used as reaction media in thermal reactions and water-soluble hexagonal-phased $NaYF_4$: Yb^{3+}; Er^{3+}/Tm^{3+} nanoparticles are formed with. Mostly, this procedure occurs in a molecular solvent (Zhang and Chen 2010; Cooper et al. 2004).

A conventional strategy for synthesis of nanocrystals is based on a simple and agreeable methodology, known as liquid–solid solution process (LSS) which provides a variation of building blocks for assembling materials in nanotechnology**.** To obtain high quality nanocrystals, basically, noble metals have been chosen for achieving good uniformity, smooth surface and self-assembly. Three phases are developed during this process—solid phase, liquid phase and solution phase. It is possible to obtain uniform noble metal nanocrystals by the moderation (reduction) of noble metal ions from interfaces of solid, liquid and solutions at various classified temperature. Here, metal linoleate acts as solid phase, ethanol–linoleic acid acts as liquid phase and water–ethanol solution with noble metal ions serves as solution phase. To generate liquid and solution phases, ethanol is a common quantity. The greatest advantage of LSS process is to produce nanocrystals having various properties such as magnetic, semiconducting, fluorescence, dielectric and applications in solid-state lasers, luminescent probes and sensors (Wang et al. 2005a).

We can divide the whole LSS process into two sections, (i) phase transfer process and (ii) phase separation process. In phase transfer process, the aqueous solution with noble metal salt conjugate with ethanol which is also in a liquid form and produce water–ethanol solution containing noble metal ions. Again phase transformation based on ion exchange occurs between sodium linoleate and the water–ethanol solution accomodating noble metal ions resulting in noble metal linoleate and finally sodium ions enter into the aqueous phase. At certain selected temperature, ethanol in both phases (liquid phase and solution phase) alleviates noble metal ions at the interfaces of solid–liquid and solid–solution phases(Wang et al. 2005b). Here, the only remaining quantity which not reacting with other chemicals is the linoleic acid, which is absorbed on the noble metal—nanocrystal surface further with the reduction process (reduction of the noble metal ions). As a result, alkyl chains are developed outside the noble–metal surface enabling them to acquire hydrophobic surfaces. In LSS process, phase separation occurs spontaneously owing to the weight of nanocrystals as well as incompatibility between their hydrophobic surfaces and hydrophilic surroundings.

In Fig. 5, TEM micrograpgs of β-NaYF$_4$: Yb, Er nanoplates (Wei et al. 2006) prepared by liquid–solid dual phase approach are shown.

5 Few Recently Developed Synthetic Strategies

Now, in the subsequent section, some of the recently developed synthetic strategies for UCNPs and their special investigations have been summarized.
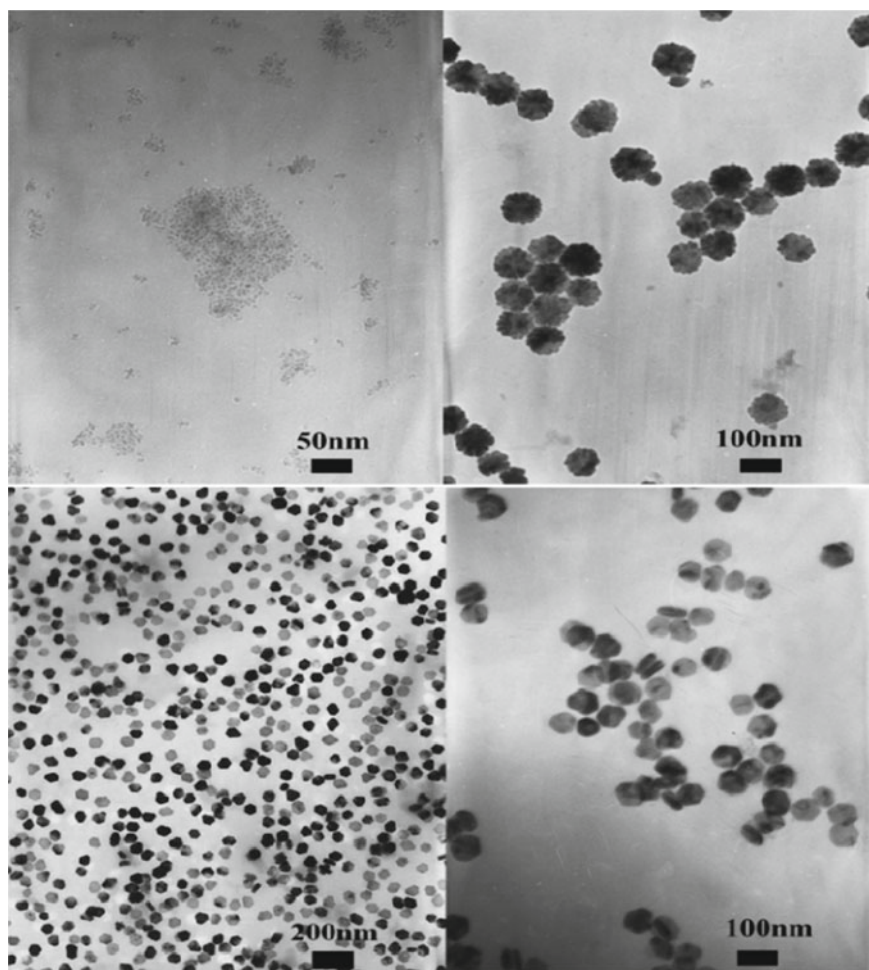
Fig. 5 TEM images of NaYF$_4$: Yb, Er UCNPs obtained at different reaction temperatures. Reported with permission (Wei et al. 2006). *Copyright* Chemistry of Materials publication

5.1 *Microwave Assisted Synthesis*

There are two leading mechanisms, dipole rotation and ionic conduction which determine the potentiality of a material for absorbing microwave radiation and transmuting it into heat**.** Though mostly, microwave-assisted synthesis was used in organic synthesis but nowadays to prepare monodispersed upconverting nanocrystals (Kubrakova and Toropchenova 2008; Zhu et al. 2004; Wang and Nann 2009; Panda et al. 2007), this method is using. Some advantages are there behind using such method, they are

(a) Convenient and reproducible method which allows preparing highly luminescent, small monodispersed nanocrystals (Wang and Nann 2009).
(b) Rapid reaction takes very less time to complete the reaction and to form luminescent nanocrystals.
(c) Provides particles having different required sizes and shapes.
(d) Hence, the polar reactants (accompanied by high microwave extinction coefficient) are excited by direct absorption of microwaves and as a result, the activation energy reduces, consequently reaction rate enhances. As outcome, lower temperature is required to perform the reactions, therefore, additional temperature in inhomogeneities is being eliminated and the leading experimental parameters (time, temperature, pressure) become easier.
(e) Growth and nucleation of resulting nanocrystals in such synthesis procedure can be distinctly described with clear explanation. Hence, growth and nucleation of nanocrystals occur in three phases, in first phase, slowly the reactant concentration increases and finally exceeds solubility, in second phase, reactant concentration extends the critical limit of super saturation, therefore, rapid nucleation is obtained and eventually this nucleation burst, reactant concentration reduces to the depletion of the solute for the growth of generated nuclei and here nucleation stage ends. In the third phase, gradually nuclei grow. Such processes follow the LaMer Mechanism. In such way, the whole reaction can be managed favourably and the resulting nanocrystals exhibit excellent monodispersity and crystallinity due to polar reactants, high microwave extinction coefficient.

5.2 Photopolymerization

Using this strategy, it is possible to induce different monomers with different desired functional properties (such as—Hydrophobic or hydrophilic, charged or neutral, chemically active or inactive) within up converting nanocrystals by coating them with thin polymer shells known as photopolymerization which utilizes internal UV or emitting visible light from them on NIR excitation. This is a simple, generic and straightforward and versatile approach to functionalize, conjugate, protect and make upconverting nanoparticles bio-compatible (Beyazit et al. 2014).

Utilization of NIR excitation in photopolymerization provides special advantages like, less probability of occurring photodamage to living cells owing to its high tissue penetration depth, ability (due to its higher wavelength) to avoid photobleaching, weak chemical stability as such difficulties arise with excitation having lower wavelength (Wang et al. 2010a, b; Chatterjee et al. 2010). With photopolymerization, upconverting nanocrystals draw some disadvantage while using in biological media as they are hydrophobic in nature and non-dispersible in nature. Therefore, after photopolymerization also their surfaces are needed to be modified and functionalized in a precisely controlled manner (Jiang et al. 2012).

5.3 Advanced and Recent Synthetic Strategies in UCNPs with Various Advanced Applications

Recently, unifying core and shell material became most attractive synthetic strategy yielding high quality and high sensitivity involving energy transfer process between Eu^{3+} and Gd^{3+} ions (Duhnen and Haase 2015). There exists a twisted relationship between upconversion efficiency and lattice geometry providing a strategy for designing the quantum efficiency of any lanthanide upconverter. This strategy has been published in literature in present day (Wisser et al. 2015). The chitosan—conjugation is the another method to increase the cell viability of upconverting nanocrystals in human breast cancer cells, in such approach upconverting nanocrystals exhibit bright upconversion fluorescence with controlled size and shape on 974 nm excitation (Ghosh 2014). Upconversion nanoparticles can also be served as luminescent nanotherometers over a wide temperature range and such nanothermometers can be processed by affiliation of liquid–solid solution hydrothermal strategy and thermal decomposition strategy and become excellent temperature sensor (Xu et al. 2015). Lanthanide-doped upconversion nanocomposites (such as—Ln^{3+}-doped $BiPO_4/BiVO_4$ nanocomposites) can also be used for photocatalysis applications. Lanthanides (e.g. Tm^{3+}) emit strong blue spectra which are transferred $BiVO_4$ resulting formation of excitations which produces reactive oxygen species. In literature survey, it has been suggested that upon NIR and solar irradiation photocatalysis activity of such resulting upconverting nanocomposites are more advantageous than the reported general nanocomposite photocatalysts. In recent past years, few advanced applications of UCNPs have been established, such as, a multifunctional nanocluster having dual compositions of gold nanorod (AuNR) and UCNPs showed applications in imaging of cancer cells and treatment. In neuroscience and engineering, stimulating deep brain neurons is an important desire. Molecularly tailored UCNPs (dendritic) have been served as less invasive optogenetic actuators to stimulate deep brain neurons (Chen et al. 2018a, b). UCNPs based theranostic system is very useful for multi-drug resistance reversing ability for chemotherapy (Chen et al. 2018a, b). A UCNP based system: $LiYF_4$: $Yb^{3+}/Tm^{3+}@SiO_2$ coated with chitosan (CH) hydrogel has become an excellent theranostic platform by controlling drug-delivery and deep-tissue imaging for several important applications, tissue engineering, bio-mapping and cellular imaging (Jalani et al. 2016). Highly specific tumour-imaging can be exhibited by the conjugate forms of Upconversion-nanoprobes with cancer cell (CC) membrane, such combined form (CC-UCNPs) represents novel materials presenting attractive class of advanced materials (Rao et al. 2016).

Table 3 Tunable morphology of UCNPs with controlling K^+ ions

Concentration of k^+ ions (in mol %)	Morphology of resulting nanocrystals	Diameter of the resulting particles
0	Spherical ($NaYF_4$)	26 nm
20	Regular hexagonal cross section (plate-like; uniform in size; $NaYF_4$)	-
40	Rectangular-like cross section ($NaYF_4$)	–
80–100	Spherical hexagonal (KYF_4)	

5.4 Investigation of Phase Transformation and Morphology Tuning in UCNPs

Phase and morphology of UCNPs can be tuned by using proper dopant ions. Zhang's group and Kal's group have been already depicted the crystal structure of such upconverting nanocrystals through K+ ions co doping (Liang et al. 2015) and there are various literature reported on the different morphologies and phases of the resulting nanocrystals (Wei et al. 2006; Yang et al. 2007; Ye et al. 2010; Dou and Zhang 2011). Phase transformation and morphology both are dependent on several experimental parameters, such as reactant's concentrations, reaction time and reaction temperature. Concentration of dopants can also play a significant role on phase transformation. For example, different concentrations of K + ion dopants in $NaYF_4$: Yb^{3+}, Er^{3+} nanocrystals display different XRD peaks. It has been reported that upto a certain limit (60 mol %) of such dopant concentration hexagonal $NaYF_4$ nanocrystals become dominant phase but beyond that limitation (when exceed 60 mol %: around 80–100 mol %) K^+ ions replace Na^+ ions and form hexagonal KYF_4 nanoparticles that mean phase transformation takes place (Liang et al. 2015). The reason behind that phase transformation is the imbalance of the intrinsic crystal structure. K^+ ions only settle in the substitution position of Na^+ ions and when number of occupying K^+ ions becomes large compared to Na^+ ions (at that moment Na^+ ions are too few), hexagonal KYF_4 appears having poor crystallinity.

Now, how the morphology of UCNPs ($NaYF_4$: Yb^{3+}, Er^{3+}) can be tuned with tuning concentration of dopant ions (K^+ ions), is shown in Table 3.

5.5 Mechanistic Investigation of Photon Upconversion

It is known, in most of the cases that the lanthanide-doped upconverting materials (ex: $NaYF_4$: Yb^{3+}, Er^{3+}) need 980 nm excitation. But this event creates problem which became a daunting challenge nowadays as absorption band of Yb^{3+} (980 nm), which acts as dopant in host lattice ($NaYF_4$), dangles with absorption band of water

molecules used in the biological sample**.** Therefore, under 980 nm excitation over-exposure of biological species results in cell death and tissue damage due to over-heating issues. To overcome such drawback, 980 nm laser excitation can be replaced by 800 nm laser excitation occurring low absorption coefficients and it is possible through use of Nd^{3+} dopant ions as sensitizer due to their favourable characteristics (As their sharp absorption bands are centred around 800 nm) (Xie et al. 2013).

6 Biological Applications of UCNPs Based on Their Immobization to Assemblies

For several biological applications, surface modification of UCNPs plays an important part for upgrading their photostability and to attach with bio-molecules. Normally, UCNPs bear a good portion of surface dopant ions. Now presence of weakly bound impurities on surface and ligands can diminish the luminescence of dopant ions due to the creation of high energy oscillations. On the other side, the excitation energy of interior ions can be dissipated non-radiatively due to their transferred energy towards the crystal-surface. As a result, the crystal field strength decreases and finally the overall UC luminescence intensity reduces abruptly. To overcome this drawback, surface modification (surface passivation and surface functionalization) is required. By surface passivation, all the dopant ions can be confined in an interior core and therefore can dominate the energy transfer towards crystal-surface. An upconversion luminescence enhancement of about 30 times was successfully carried out by one research group with 1.5 nm thick $NaYF_4$ shell on 8 nm sized NaYF4: Yb/Tm nanocrystals (Mai et al. 2007). By varying the thickness of the shell, UC luminescence efficiency can be well tuned and by several research groups (Park et al. 2009; Yi and Chow 2007; Lu et al. 2008; Chen et al. 2008), this process has been successfully explained by immobizing the nanocrystals (UCNPs) inside a coated shell. Besides, surface passivation, surface functionalization is also an important part to use those UCNPs in biomedical and bio-detection. Hence, by ligand-exchange technique $NaYF_4$: Yb/Er nanoparticles can be made water soluble by utilizing bi-functional organic molecules which replaced amine ligands and modified the crystal surfaces as water-soluble carboxyl functionalised surface(Wang et al. 2010a, b).

Moreover, the immobilization concept of UCNPs has been confirmed by their several biological applications via bio-conjugate chemistry as these techniques are, while applied to UCNPs, capable of immobilization to bio-assemblies. Based on the immobilization concept, some specific bio-applications of UCNPs are discussed below.

In cells and small animals, the innovative UCNPs have been considered to be promising molecular probes for optical imaging. In 2013, Grebenik et al. group reported UCNP-labeled cancer lesion where the synthesized nanoparticles were capped with amphiphilic polymer. Further, mini-antibodies (scFv4D5) were attached onto UCNPs for allowing their specific binding to the human cells. As a result, the

UCNP based bio-complexes showed high specific immobilization on human breast adenocarcinoma cells SK-BR-3 (Grebenik et al. 2013).

In 2017, Shikha et al. group developed a UCNPs-based multiplexed detection system to encode PEGDA microbeads and to label antibodies. Hence, the multicolour codes were produced by mixing green and red emissions from UCNPs whereas its blue emissions were used to label antibody. By immobilizing probe antibodies on red-UCNPs and anti-human C reactive protein (hCRP) on green UCNPs, specific capturing of human serum albumin (HAS) protein and multiplexed detection of HCRP and HSA proteins were done, respectively (Shikha et al. 2017).

RGDS and TAT conjugated $NaYF_4$: Yb^{3+}/Er^{3+}, SiO_2 nanoparticles were targeted in HeLa cells by in vitro study where RGDS-conjugated probes were confined on cell-plasma membrane for the specific binding between the conjugated peptides and integrins. This application also clearly confirms the immobilization behaviour of UCNPs (Kostiv et al. 2016).

In 2016, T. sang et al. group proposed a conjugated system of $BaGdF_5$: Yb/Er UCNPs and AuNPs to increase the effective detection of limit for target Ebola virus from picomolar level to femtomolar level. The enhancement of this ultrasensitive detection exhibited a great potential for practical application due to the specificity between nanoprobes and Ebola virus oligonucleotides (Tsang et al. 2016).

The bare monodisperse UCNPs were immobilized for developing bio-sensing surface. Further, for developing bio-assays and bio-sensors, a high immobilization density for UCNPs was reported by Doughan et al. group in 2014 and the reported immobilization density was calculated of about ~1.3×10^{11} UCNP cm^{-2} where PEA—UCNPs were immobilized on functionalized coverslips (Doughan et al. 2014).

PEG-b-PAAc was immobilized on erbium-ion-doped Y_2O_3 [Y_2O_3: Er] particle—surface to enhance its dispersion and prevent adsorption. Further, co-immobilization of PEG-b-PAAc and BSA occurred due to the protein installation on particle—surface (Kamimura et al. 2008).

According to previous report (Freitag et al. 2019), the immobilized photoredox catalyst based on $NaYF_4$ nanoparticles was capable for in vivo applications. The immobilized system successfully performed under 980 nm NIR source.

In particular, based on the immobilization strategies, upconverting nanoparticles have given a huge response in bio-applications. In the applications of cellular and molecular biology, several bio-probes (Green fluorescent protein, (GFP), organic dyes) are used for identification of different bio-molecules, which is an indispensable step. To develop the sensitivity of some technical and analytical devices used in bio-field utilization of such available probes is a crucial step as they improve the efficiency of detection. Still some drawbacks (such as weak photostability of probes, measuring cell response having instrumental problem with resolution) are there with such bio-probes which limit their biological applications. To overcome such drawbacks nano particles with protein-imaging, nucleic acid-detection with nanodiamonds (Faklaris et al. 2008; Chang et al. 2008), metallic nanoparticles, dye-doped silica particles have been already discovered. As nanoparticles consist of a large number of ions, single particle and single molecule identification is favourable owing to large surface area implanting of different targeting groups at the surface and it can be done comfortably.

For more advanced applications, recently, RE-based nanoparticles have been proved to be most optimistic materials (Vetrone and Capobianco 2008) due to their especial properties such as long lifetimes, narrow emission lines, high photostability, low cytotoxicity and simplistic functionalization procedures which make them highly bio-compatible and recognizable compared with other Nano particles. In magnetic resonance imaging (MRI) due to their high magnetic moment and inoxidant detection applying reverse oxidoreduction process, the requirement of UCNPs is noticeable. In MRI, RE ions can be regarded as a powerful contrast agent. To fabricate nanoparticles (e.g. silica particles) (Shao et al. 2011) as high bio-compatible material various chemical properties could be induced by inducing different rare earth compounds as dopant-agent. Mesoporous silica shell nanocomposites used for bimodal imaging is the best example of such nanoparticles doped with RE compounds.

Surface modification or surface functionalization and bio-conjugation are crucial steps after synthesis known as post synthesis method before using in the biological field. Every nanoparticle has a certain surface chemistry and specific physical and chemical properties to govern nucleation or growth of resulting particles as well as to control their dispersion in the solvent used. Generally, after synthesis of upconversion nanoparticles, due to the presence of some organic ligands capped with them, they become non-dispersible which are not suitable for bio-applications. For using in different biomedical applications, upconversion nanoparticles based bio-probes are fabricated to functionalize their surfaces to ensure good dispersion in biological media and to uncover specific organic or bio-organic groups from the particles and to make them appropriate for accurate targeting receptor sites (Fig. 6).

Ensuring the stability of hydrophobic nanoparticles in aqueous media is a necessary condition in biological applications and that can be processed by applying
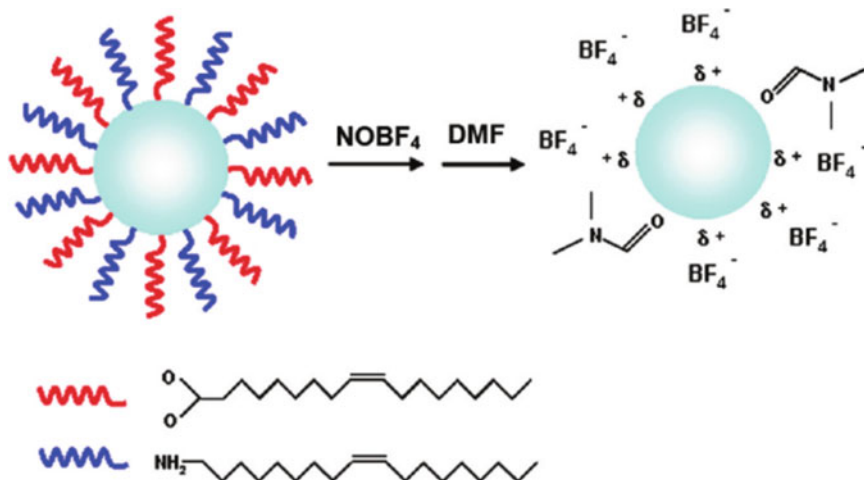

Fig. 6 Illustration of ligand-exchange with NOBF$_4$. Reproduced with permission (Dong et al. 2011). *Copyright* Journal of the American Chemical Society publication

diverse functional strategies which are described by following: In Ligand exchange, the original ligands are replaced by other molecules Citrate, PVP, PAA, TGA, PEG and finally become stable dispersible in biological media (Figs. 7, 8) (Boyer et al. 2010; Dong et al. 2011).

By direct surface grafting of molecules and polymer encapsulation method, several reactive groups (e.g. amino, thiols, etc.) can be attached on the resulting particle-surface (Nichkova et al. 2005). Streptavidin, antibodies are some bio-molecules with which nanoparticles can be directly coupled. Because of surface hydroxyl groups acting as a coupling agent with silanes present in the oxide nanoparticles, by silica and organosilane coating functionalization can be done in a quite simple way.

Layer by layer assembly is another propitious method for surface modification, obtaining by sequential adsorption of oppositely charged polyelectrolytes on particle surface. Such sequential adsorption (i.e. sequential deposition of PAA and PAH) has
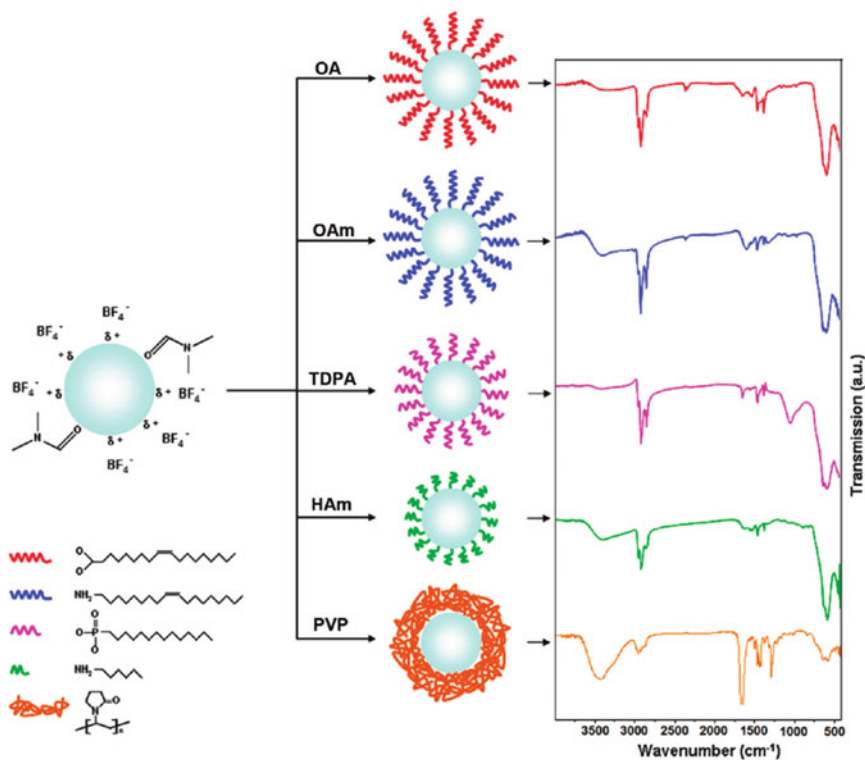

Fig. 7 Illustration of secondary ligand-exchange exhibiting surface functionalization of BF$_4$—modified Fe$_3$O$_4$ nanocrystals with several capping molecules and their corresponding FTIR spectra. Reproduced with permission (Dong et al. 2011). *Copyright* Journal of the American Chemical Society publication
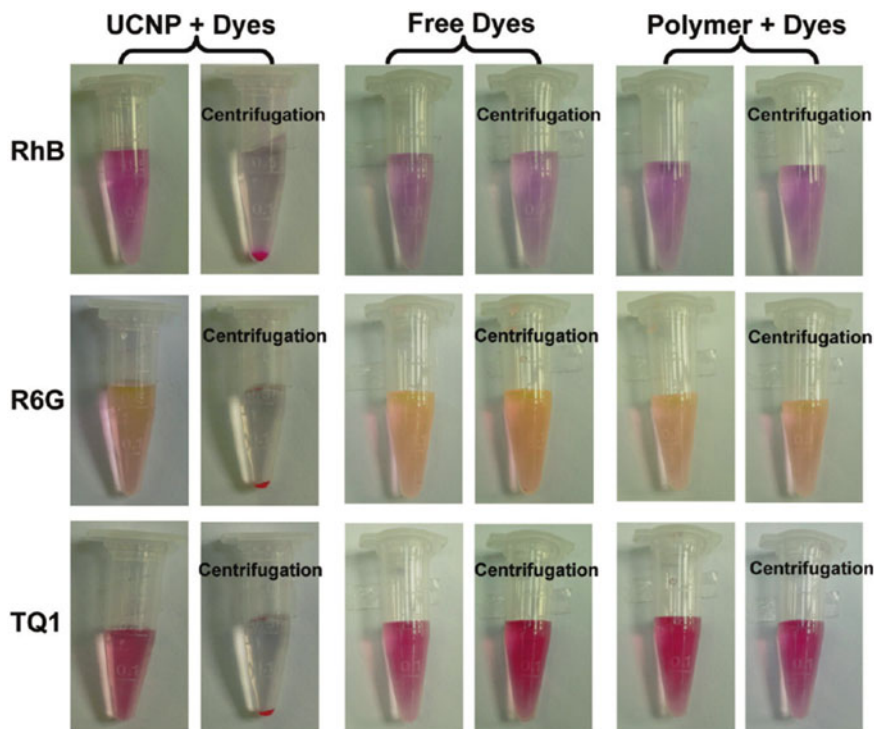
Fig. 8 UCNP/dye—images captured while centrifuged (before/after). UCNPs and dye molecules appeared as precipitate by centrifugation force while supernatant part appeared as clear colourless solutions in containers. Precipitation was not observed while centrifugation occurred with free dye molecules or PEG-PMHC$_{18}$+dye mixtures. These images indicated that UCNP-surface adsorbed three types of dye molecules rather than their encapsulation in UCNP-dye complexes by amphiphilic PEG-PMHC$_{18}$ polymer. Reproduced with permission (Cheng et al. 2011a, b). *Copyright* The Journal of Physical Chemistry C publication

been already observed in literature providing superior mechanical stability and a well-ordered NIR to visible upconversion luminescence. But here some drawbacks which limits its requirement as this method is only applicable for hydrophilic nanocomposites and time consuming, many washing steps are needed during that assembly. Surface silanization is the most frequently used surface functionalization method requiring the growth of silica shell on upconversion nanoparticles. The importance of this process is the use of silica as silica is considered to be bio-compatible and porosity is easily controllable. The encapsulation of silica layer on UCNPs is still under investigation to modify the difficulties(such as, most of the reagents used are toxic in nature, therefore before starting that encapsulating process they should be detached carefully) introduced by silica layer and other reagents used in such encapsulating process. If we desire to use silica encapsulation in FRET-bio-sensors, the increasing shape and size of the resulting particles will create difficulties during

experiment. To suppress those difficulties, two approaches are useful, one is Stober method and other one is reverse microemulsion route.

Although controlling that Stober method is quite difficult and takes long time, thus it is straightforward and fruitful path in the presence of ethanol and ammonia, whereas reverse micro emulsion route can be controlled in the presence of homogeneous mixture of water, oil, surfactant and TEOS to dominate the increasing thickness, size and shape of the additional silica layer. One user-friendly surface modification for providing hydrophilic nanoparticles as well as hydrophobic layer for loading hydrophobic molecules(Drug, Dyes) is the Host–Guest Self-assembly method which has a lot of advantages over the other methods due to its simplicity and efficiency. As this procedure is very fast, over 95% of nanoparticles can be transferred to water using reagents (Liu et al. 2010).

We have already discussed that by proper surface modification, it is possible to affix various functional groups with UCNPs, like-carboxyl, amine and thiol groups. After such functionalization, these UCNPs with several attached groups can be decorated with various biomolecules which can contribute bio-identification of other targeted cells. There are diverse approaches of bio-conjugation. Among these, the greatest advantageous method is Direct Physisorption. This method occurs via non-covalent force of biomolecules. The activity of proteins and quantum yield of resulting nanoparticles remain unchanged after that bio-conjugation. Assisted Physisorption is of other crucial importance in bio-conjugation and uses pre-bound molecules and occurs by non-covalent coupling of two molecules. This is an essential method in bio-specificity and bio-sensitivity due to the proper orientation of molecules. By direct chemical coupling of bio-molecules also bio-conjugation can be induced in UCNPs. But this method cannot be controlled easily as other complex processes such as gel electrophoresis is required for separation after completion of this process. In UCNPs' surface modification with biotin-protein bond (streptavidin-coupling) can be useful for various biomedical application, which is the strongest and most stable non-covalent interaction.

A general overview on UCNPs applications is highlighted below.

6.1 DNA and Protein Detection

It has become a great challenge for application of RE-based nanoparticles for DNA and protein detection. Implementation of such nanoparticles in DNA detection is based on two strategies, DNA sensitive nanoparticles and DNA fragments nanoparticles. Here, we are describing one by one.

In case of the first approach, DNA concentration can be computed using fluorescent upconversion nanoparticles (Wang et al. 2009) which can be comparable to conventional measurement executed by spectrophotometer. As per optical properties, we already know that fluorescence property UCNPs make them valuable for their applications. Now, due to some specific dopant ions (such as: Ce^{3+}, Tb^{3+} dopants in LaF_3, fluorescence occur due to Tb^{3+} dopant ions) and their transitions in energy

levels, the fluorescence of upconversion nanoparticles become very prominent and in the presence of DNA, the amount of fluorescence can be quenched by the generating generation of hydrogen bonds between DNA and nanoparticle. As a result, the energy can be transferred from excited dopant ions (Tb^{3+} in the given example above) to DNA. Finally, it is possible to quantify DNA concentration by determining the corresponding fluorescence intensity. In the second approach, to study mRNA pattern, DNA microarrays are used extensively for which there are two requirements, one for hybridization of probe DNA strands and other for labelling target DNA fluorescently. In such technology, also fluorescent intensity quantifies the DNA fragments in each probe. Later, other advantageous technology comparable to the depicted one, reported in literature according to which for labelling, target DNA is combined with UCNPs (e.g. Y_2O_2S: Yb, Er) and finally, it is possible to measure the concentration of the target DNA. The later one is superior technology than the former for determining DNA concentration, as the former technology weakly express mRNA.

UCNPs can also be used for diagnosis diseases such as Fe_3O_4/Gd_2O_3: Eu nanoparticles where Fe_3O_4 construct the magnetite core and Gdo_3 constructs the shell of the nanoparticles and the dopant ion Eu^{3+} make the particle fluorescent by transferring energy. Now, it is known, detection of single nucleotide polymorphisms (SNPs) is very significant phenomenon for recognition of various diseases like polycystic kidney disease (PKD) by using reverse transcription polymerase chain reaction (RT-PCR) but due to some shortcoming vis a vistime consuming and expensive, it cannot be applied in the biomedical field. In the present days, to solve these problems successfully, UCNPs have been introduced to detect SNPs (Son et al. 2008). In that approach, rare earth-based nanoparticles are used in such a systematic manner, that they can combine both magnetism and fluorescence properties to provide a strong and effective analysis.

Europium-doped gadolinium oxide nanoparticles can also be used for detection of protein micropatterns for coupling with antibodies rather than organic dyes. Such rare earth-based nanoparticles with organic cores have also been successfully utilized in immunoassays. As a result, sensitivity of the whole complex can be improved in the presence of rare earth-based UCPN nanoparticles.

6.2 Fluorescent Resonant Energy Transfer (FRET)

FRET has wide applications (among which protein–protein interaction is the most significant phenomenon with the usage of FRET) in biomedical field using other materials. For protein–protein interaction, one protein (labelled with fluorophore) acts as donor and other one acts as acceptor (labelled with fluorophore) using that fluorescence energy transfer method according to which an efficient energy is being transferred from donor to acceptor and as outcome detection of fluorescence become possible providing the basic principle of FRET process. If FRET can be done in the presence of lanthanide systems, then easily such nanoparticles can be served as donors, which gives some effective and favoured conditions like prevention from

direct excitation, limitations in overlapping spectra and their easy separation, long lifetimes of excited state and less probability of photobleaching and there are certain reasons why lanthanide nanoparticles were taken in FRET experiment. Hence, the lanthanide systems with the large stokes shift permit excitation having shorter wavelength than the absorption by acceptor to prevent direct excitation and UCNPs with large anti-stokes shift permits excitation at much higher wavelength than the emission by acceptor to get a clean detection from FRET. Secondly, due to narrow emission spectrum occurred by lanthanide nanoparticles, there is a very less chance of overlapping between them and acceptor emission-spectrum. Thirdly, as lanthanide systems provide excited states having long lifetime, so conducts acceptor emission with longer time and as a result separation in time-resolved experiments occurs easily. Utilizing that longer-scale phenomenon, it is possible to apply quantum dots as acceptors in FRET applications.

Advantages of upconversion nanoparticles as donors in FRET application make them unique in biomedical applications. Most of the upconverting nanoparticles are co-doped with Er^{3+} and Yb^{3+} and gives remarkable fluorescence which make them an excellent donors having interesting potential in FRET applications. Protein detection with the help of nanoparticles is possible by coating (example of such coating, agent-streptavidin), mixing (example of such mixing, agent-biotinylated protein) and labelling (example of such labelling, compound-fluorescent acceptor) in a precisely controlled manner so that after IR excitation of donors, a clear detection of fluorescence becomes possible.

6.3   *In Vivo and in Vitro Biomedical Application*

Recently, lanthanide-doped UCNPs have gathered much attention in biomedicine. In 2012, Liang Cheng et al. showed in vivo imaging of UCNPs in his experiment (Cheng et al. 2010).Auto fluorescence of the UCL imaging with long exposure time allows in vivo detection of UCNPs. UCL emission spectra of different nanoparticles can be controlled with our requirement in biological systems by altering the concentration of the lanthanide dopant ions used during synthesis and this process is essential in multicolour vivo UCL imaging with organic dyes through hydrophobic force (Fig. 8) (Cheng et al. 2011a, b). In tumour diagnosis, UCL imaging plays significant role by tumour targeted molecular imaging using UCNP-based nanoprobes. Basically for synthesis of such nanoprobes, conjugating polymer-coated UCNPs are used, the aim of which is to bind different cancer cells having high specificity explore a new challenge in future studies and experiments. UCNPs have also been successfully synthesized to utilize in vitro applications such as labelling and tracking rabbit bone marrow mesenchymal stem cells (rBMSCs) (Ma et al. 2016). In 2008, both in vivo and in vitro studies were performed using aqueous dispersible rare earth-ion (Tm^{3+} and Yb^{3+}) co-doped fluoride ($NaYF_4$) nanocrystals, where upconversion process provided deeper penetration into biological specimen resulting high contrast optical imaging (Nyk et al. 2008). In 2011, in vitro and in vivo imaging was implemented by

utilizing 915 nm LASER excited $NaYbF_4$ UCNPs co-doped with $Tm^{3+}/Er^{3+}/Ho^{3+-}$ rare earth elements to avoid overheating irradiation caused by 980 nm laser excitation source.

Hence, the experimental results were successfully investigated and showed very high contrast upconversion bio-imaging and a successful performance for in vivo imaging where highly stable UCNPs encapsulated with DSPE-mPEG-5000 were injected into mice (Zhan et al. 2011). For delivering in vitro and in vivo operations, caged UCNPs are being served as excellent platforms to improve targets along with reduction of side effects from chemotherapy by using them as NIR-triggered targets (Chien et al. 2013).

To overcome the drawbacks of single imaging approach, nowadays, the multimodal imaging has gained enormous recognition in biomedical applications. There are several approaches (Zhu et al. 2012; He et al. 2011; Xing et al. 2012) to progress UCNPs based nanoprobes for multimodal bio-imaging. UCNPs as well as their nanocomposites can be utilized to fabricate such multimodal imaging bio-probes. Also in the field of cell labelling and in vivo tracking, UCNPs are sensible enough. Recently, investigation of mesenchymal stem cells (MSCs) has been started owing to their ability of recognition various types of cells (e.g. bone) under certain circumstances in various potential applications in bio-field such as in immunotherapy and gene therapy.

6.4   Medicinal and Remedial Applications

In present days, UCNPs and their composites can be considered as therapeutic agent in cancer treatment, drug gene delivery and for photodynamic therapy due to their various unique properties and functions as well as imaging capability. For imaging and therapy, chemotherapy drug molecules could be delivered with loading of UCNPs. For drug releasing system, polymer-coated UCNPs can also be used. For treatment of various gene-related diseases, gene therapy with gene encoding DNA or RNA has become a challenging matter. UV light emitted from UCNPs activates definite gene expression by operating DNA and RNA, though depth of penetration. The therapeutic efficiency is very high in case of UCNPs with NIR excitation compared with UCNPs with UV light and such PDT based on UCNPs exhibited greater potential in treatment of cancers as well as suppression of the size of large internal tumours.

To treat cancer diseases, Photodynamic Therapy (PDT) is a non-invasive and effective medical method which uses photosensitizers (PDT drugs) and light irradiation and they interact with molecular oxygen. There are several approaches to originate PDT reagents like silica encapsulation, polymer encapsulation, and hydrophobic interaction. At first, photosensitizers are activated with light and as a result, cytotoxic reactive oxygen species are formed and persuade required cell death (Park et al. 2012). Assembly of oxygen molecules are influenced by the energy transfer process

from excited UCNPs relying on the spectral overlapping of donor and acceptor impurities in host lattice. There are two factors that quantify photodynamic therapy, one is high energy transfer efficiency and the other is large production of singlet oxygen and these two phenomenons are related with high stability of originally loaded photosensitizers in UCNPs. For good energy transfer process, non-covalent form of UCNP-PS is not ideal as this provides low loading efficiency and finally small production of singlet oxygen. For that a covalent conjugating of UCNPs (NaYF$_4$, Yb^{3+}, Eb^{3+}), photosensitizer and target molecule strategy can be adopted. For singlet oxygen and high fluorescence intensity production, a multifunctional upconversion nanoplatform has been already expanded on the basis of a particular energy transfer from UCNPs to photosensitizer for synchronous imaging and therapy (Fig. 9) (Liu et al. 2012). The therapeutic consequences of UCNP-PS compound for animal studies and cellular level have been already reported(Park et al. 2012). It has been reported in literature that for in vitro cancer cell destroying, mesoporous silica-coated UCNP-PS combination shows an interesting and encouraging result (Guo et al. 2010). Gu's group has revealed the uses of UCNP-PS nanocomplexes in the field of in vivo PDT (Cui et al. 2012). For in vitro and in vivo tracking, UCNPs have been used to designate stem cells by different groups (Wang et al. 2012).
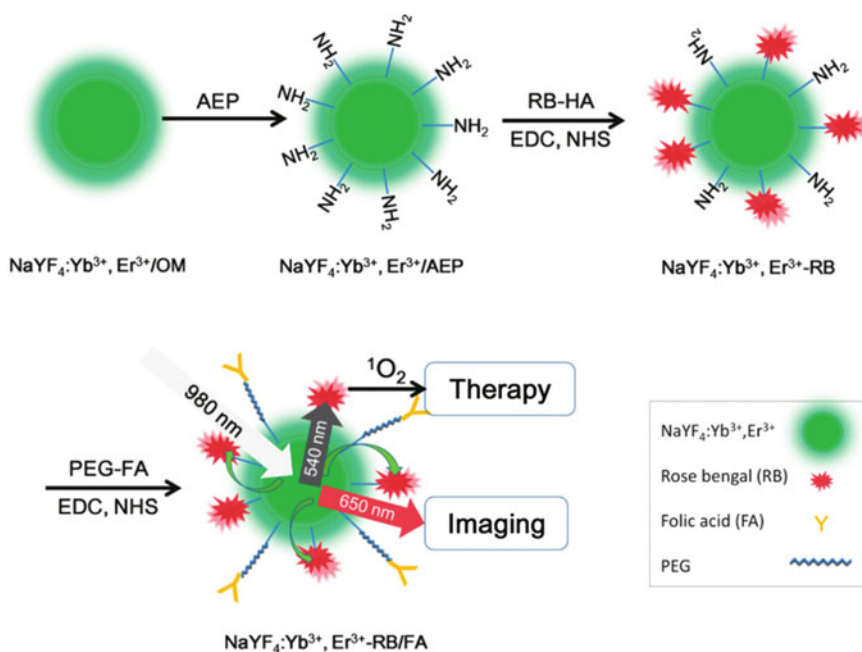

Fig. 9 Covalent conjugation of NaYF$_4$: Yb^{3+}, Er^{3+} UCNPs, photosensitizer (RB), target molecule (FA). Reproduced with permission (Liu et al. 2012). *Copyright* ACS Nano publication

7   Conclusions

This review explores recent developments of UCNPs along with a detailed survey and as application part, it focuses in bio-fields (imaging and therapy). Though there are tremendous amount of applications and a number of exciting aspects have been reported in literatures since past few years on this field but still many challenges are ahead especially in imaging and therapy.

With reducing the sizes of UCNPs, the quantum yield became lower which limits their use in various nano-probes. Later, several research groups modified the synthesis and production of UCNPs to increase their yield under continuous wave-excitation sources but still future efforts are required to make them useful for enormous number of in vivo applications. The long-term toxicity of RE-doped UCNPs is another perturbation. Though, bio-compatible coating-based UCNPs (NaYF$_4$) appeared to be safer to cells (with precise concentrations) compared to bared UCNPs, but, still other factors like their interactions with immune systems, interference with the reproductive system, whether the toxicity is affecting for next generation applications, that are still not known for which more number of systematic investigations are demanded. The effects of surface functionalization and sizes of UCNPs on in vivo behaviours are required to improve in reducing certain potential toxicity. Though imaging and therapies based on UCNPs and their different nanocomposites have been revealed in previous literatures, to achieve synergistic therapeutic effects and realize real-time scanning of treatment development, an improved design of UCNPs based on novel multifunctional agents is needed further for simultaneous medical diagnosis and cancer treatment.

References

Auzel F (2004) Upconversion and Anti-Stokes processes with f and d Ions in solids. Chem Rev 104:139–174

Barnes WL, Dereux A, Ebbesen TW (2003) Surface plasmon subwavelength optics. Nature 424:824–830

Beyazit S, Ambrosini S, Marchyk N (2014) Versatile synthetic strategy for coating Upconverting nanoparticles with polymer shells through localized photopolymerization by using the particles as internal light sources. Angew Chemie Int Ed 53:8919–8923

Boyer JC, Cuccia AL, Capobianco J (2007) Synthesis of colloidal upconverting NaYF 4: Er 3+/Yb 3+ and Tm 3+/Yb 3+ monodisperse nanocrystals. Nano Lett 7:847–852

Boyer JC, Manseau MP, Murray JI, van Veggel FCJM (2010) Surface modification of Upconverting NaYF$_4$ nanoparticles with PEG−Phosphate ligands for NIR (800 nm) biolabeling within the biological window. Langmuir 26:1157–1164

Boyer JC, Vetrone F, Cuccia LA, Capobianco JA (2006) Synthesis of colloidal Upconverting NaYF$_4$ nanocrystals doped with Er^{3+}, Yb^{3+} and Tm^{3+}, Yb^{3+} via thermal decomposition of lanthanide trifluoroacetate precursors. J Am Chem Soc 128:7444–7445

Chang IP, Hwang KC, Chiang CS (2008) Preparation of fluorescent magnetic nanodiamonds and cellular imaging. J Am Chem Soc 130:15476–15481

Chatterjee DK, Gnanasammandhan MK, Zhang Y (2010) Small Upconverting fluorescent nanoparticles for biomedical applications. Small 6:2781–2795

Chatterjee DK, Rufaihah AJ, Zhang Y (2008) Upconversion fluorescence imaging of cells and small animals using lanthanide doped nanocrystals. Biomaterials 29:937–943

Chatterjee DK, Yong Z (2008) Upconverting nanoparticles as nanotransducers for photodynamic therapy in cancer cells. Nanomedicine 3:73–82

Chen S, Weitemier AZ, Zeng X (2018) Near-infrared deep brain stimulation via Upconversion nanoparticle–mediated optogenetics. Science 359:679–684

Chen X, Sun J, Zhao H (2018) Theranostic system based on NaY(Mn)F_4:Yb/Er Upconversion nanoparticles with multi-drug resistance reversing ability. J Mater Chem B 6:3586–3599

Chen Z, Chen H, Hu H (2008) Versatile synthesis strategy for carboxylic acid−functionalized Upconverting nanophosphors as biological labels. J Am Chem Soc 130:3023–3029

Cheng L, Yang K, Li Y (2011) Facile preparation of multifunctional Upconversion nanoprobes for multimodal imaging and dual-targeted photothermal therapy. Angew Chemie Int Ed 50:7385–7390

Cheng L, Yang K, Shao M (2011) Multicolor in vivo imaging of Upconversion nanoparticles with emissions tuned by luminescence resonance energy transfer. J Phys Chem C 115:2686–2692

Cheng L, Yang K, Zhang S (2010) Highly-sensitive multiplexed in vivo imaging using pegylated Upconversion nanoparticles. Nano Res 3:722–732

Chien YH, Chou YL, Wang SW (2013) Near-infrared light photocontrolled targeting, bioimaging, and chemotherapy with caged Upconversion nanoparticles in vitro and in vivo. ACS Nano 7:8516–8528

Cooper ER, Andrews CD, Wheatley PS (2004) Ionic liquids and eutectic mixtures as solvent and template in synthesis of zeolite analogues. Nature 430:1012–1016

Cui S, Chen H, Zhu H (2012) Amphiphilic chitosan modified Upconversion nanoparticles for in vivo photodynamic therapy induced by near-infrared light. J Mater Chem 22:4861–4873

Dong A, Ye X, Chen J (2011) A generalized ligand-exchange strategy enabling sequential surface functionalization of colloidal nanocrystals. J Am Chem Soc 133:998–1006

Dou Q, Zhang Y (2011) Tuning of the structure and emission spectra of Upconversion nanocrystals by alkali ion doping. Langmuir 27:13236–13241

Doughan S, Han Y, Uddayasankar U, Krull UJ (2014) Solid-phase covalent immobilization of Upconverting nanoparticles for biosensing by luminescence resonance energy transfer. ACS Appl Mater Interfaces 6:14061–14068

Downing E, Hesselink L, Ralston J, Macfarlane R (2006) A three-color, solid-state, three-dimensional display. Science 273:1185–1189

Duhnen S, Haase M (2015) Study on the intermixing of core and shell in $NaEuF_4$/$NaGdF_4$ core/shell nanocrystals. Chem Mater 27:8375–8386

Ehlert O, Thomann R, Darbandi M, Nann T (2008) A four-color colloidal multiplexing nanoparticle system. ACS Nano 2:120–124

Eustis S, El-Sayed MA (2006) Why gold nanoparticles are more precious than pretty gold: Noble metal surface plasmon resonance and its enhancement of the radiative and nonradiative properties of nanocrystals of different shapes. Chem Soc Rev 35:209–217

Faklaris O, Garrot D, Joshi V (2008) Detection of single photoluminescent diamond nanoparticles in cells and study of the internalization pathway. Small 4:2236–2239

Feng X, Sayle DC, Wang ZL (2006) Converting Ceria polyhedral nanoparticles into single-crystal nanospheres. Science 312:1504–1508

Freitag M, Moller N, Ruhling A (2019) Photocatalysis in the dark: near-infrared light driven photoredox catalysis by an upconversion nanoparticle/photocatalyst system. Chem Photo Chem 3:24–27

Ghosh OSN (2014) Chitosan conjugation: A facile approach to enhance the cell viability of LaF3: Yb, Er Upconverting nanotransducers in human breast cancer cells. Carbohydr Polym 121:302–308

Grebenik EA, Nadort A, Generalova AN (2013) Feasibility study of the optical imaging of a breast cancer lesion labeled with Upconversion nanoparticle biocomplexes. J Biomed Opt 18:1–11

Guo H, Qian H, Idris NM, Zhang Y (2010) Singlet oxygen-induced apoptosis of cancer cells using Upconversion fluorescent nanoparticles as a carrier of photosensitizer. Nanomed Nanotechnol Biol Med 6:486–495

Hampl J, Hall M, Mufti NA (2001) Upconverting phosphor reporters in immunochromatographic assays. Anal Biochem 288:176–187

He M, Huang P, Zhang C (2011) Dual phase-controlled synthesis of uniform lanthanide-doped $NaGdF_4$ Upconversion nanocrystals via an OA/Ionic liquid two-phase system for in Vivo dual-modality imaging. Adv Funct Mater 21:4470–4477

Heer S, Kompe K, Gudel HU, Haase M (2004) Highly efficient multicolour Upconversion emission in transparent colloids of lanthanide-doped $NaYF_4$ Nanocrystals. Adv Mater 16:2102–2105

Idris NM, Gnanasammandhan MK, Zhang J (2012) In vivo photodynamic therapy using Upconversion nanoparticles as remote-controlled nanotransducers. Nat Med 18:1580–1585

Jackson SD (2004) Cross relaxation and energy transfer Upconversion processes relevant to the functioning of 2 μm Tm^{3+}-doped silica fibre lasers. Opt Commun 230:197–203

Jalani G, Naccache R, Rosenzweig DH (2016) Photocleavable hydrogel-coated Upconverting nanoparticles: a multifunctional theranostic platform for NIR imaging and on-demand macro-molecular delivery. J Am Chem Soc 138:1078–1083

Jiang G, Pichaandi J, Johnson NJJ (2012) An effective polymer cross-linking strategy to obtain stable dispersions of upconverting $NaYF_4$ nanoparticles in buffers and biological growth media for biolabeling applications. Langmuir 28:3239–3247

Joubert MF (1999) Photon avalanche Upconversion in rare earth laser materials. Opt Mater (Amst) 11:181–203

Kamimura M, Miyamoto D, Saito Y (2008) Preparation of PEG and protein co-immobilized Upconversion nanophosphors as near-infrared biolabeling materials. J Photopolym Sci Technol 21:183–187

Kim WJ, Nyk M, Prasad PN (2009) Color-coded multilayer photopatterned microstructures using lanthanide (III) ion co-doped $NaYF_4$ nanoparticles with Upconversion luminescence for possible applications in security. Nanotechnology 20:185301

Kostiv U, Kotelnikov I, Proks V (2016) RGDS- and TAT-conjugated Upconversion of $NaYF_4$: Yb^{3+}/Er^{3+} & SiO_2 nanoparticles: in vitro human epithelioid cervix carcinoma cellular uptake, imaging, and targeting. ACS Appl Mater Interfaces 8:20422–20431

Kramer KW, Biner D, Frei G (2004) Hexagonal sodium yttrium fluoride based green and blue emitting upconversion phosphors. Chem Mater 16:1244–1251

Kubrakova IV, Toropchenova ES (2008) Microwave heating for enhancing efficiency of analytical operations (Review). Inorg Mater 44:1509–1519

Li C, Quan Z, Yang J (2007) Highly uniform and monodisperse β-$NaYF_4$: Ln^{3+} (Ln = Eu, Tb, Yb/Er, and Yb/Tm) hexagonal microprism crystals: hydrothermal synthesis and luminescent properties. Inorg Chem 46:6329–6337

Li LL, Zhang R, Yin L (2012) Biomimetic surface engineering of lanthanide-doped upconversion nanoparticles as versatile bioprobes. Angew Chemie Int Ed 51:6121–6125

Liang ZQ, Zhao SL, Cui Y (2015) Phase transformation and morphology tuning of β-$NaYF_4$: Yb^{3+}, E^{r3}+ nanocrystals through K^+ ions codoping. Chinese Phys B 24:37801

Lim SF, Riehn R, Ryu WS (2006) In vivo and scanning electron microscopy imaging of Upconverting nanophosphors in caenorhabditis elegans. Nano Lett 6:169–174

Liu K, Liu X, Zeng Q (2012) Covalently assembled NIR nanoplatform for simultaneous fluorescence imaging and photodynamic therapy of cancer cells. ACS Nano 6:4054–4062

Liu Q, Li C, Yang T (2010) "Drawing" Upconversion nanophosphors into water through host–guest interaction. Chem Commun 46:5551–5553

Liu Y, Lu Y, Yang X (2017) Amplified stimulated emission in upconversion nanoparticles for super-resolution nanoscopy. Nature 543:229–233

Lu Q, Guo F, Sun L (2008) Silica-/titania-coated Y2O$_3$: Tm^{3+}, Yb^{3+} nanoparticles with improvement in Upconversion luminescence induced by different thickness shells. J Appl Phys 103:123533

Ma Y, Ji Y, You M (2016) Labeling and long-term tracking of bone marrow mesenchymal stem cells in vitro using NaYF$_4$: Yb^{3+}, E^{r3}+ Upconversion nanoparticles. Acta Biomater 42:199–208

Mader HS, Kele P, Saleh SM, Wolfbeis OS (2010) Upconverting luminescent nanoparticles for use in bioconjugation and bioimaging. Curr Opin Chem Biol 14:582–596

Mai HX, Zhang YW, Si R (2006) High-quality sodium rare-earth fluoride nanocrystals: controlled synthesis and optical properties. J Am Chem Soc 128:6426–6436

Mai HX, Zhang YW, Sun LD, Yan CH (2007) Highly efficient multicolor up-conversion emissions and their mechanisms of monodisperse NaYF$_4$: Yb, Er core and core/Shell-structured nanocrystals. J Phys Chem C 111:13721–13729

Mi C, Tian Z, Cao C (2011) Novel Microwave-assisted solvothermal synthesis of NaYF$_4$:Yb, Er Upconversion nanoparticles and their application in cancer cell imaging. Langmuir 27:14632–14637

Nichkova M, Dosev D, Gee SJ (2005) Microarray immunoassay for phenoxybenzoic acid using polymer encapsulated Eu: Gd$_2$O$_3$ nanoparticles as fluorescent labels. Anal Chem 77:6864–6873

Nyk M, Kumar R, Ohulchanskyy TY (2008) High contrast in vitro and in vivo photoluminescence bioimaging using near infrared to near infrared up-conversion in Tm^{3+} and Yb^{3+} doped fluoride nanophosphors. Nano Lett 8:3834–3838

Panda AB, Glaspell G, El-Shall MS (2007) Microwave Synthesis and optical properties of uniform nanorods and nanoplates of rare earth oxides. J Phys Chem C 111:1861–1864

Park Y, Kim HM, Kim JH (2012) Theranostic probe based on lanthanide-doped nanoparticles for simultaneous in vivo dual-modal imaging and photodynamic therapy. Adv Mater 24:5755–5761

Park YI, Kim JH, Lee KT (2009) Nonblinking and nonbleaching upconverting nanoparticles as an optical imaging nanoprobe and T1 magnetic resonance imaging contrast agent. Adv Mater 21:4467–4471

Rao L, Bu LL, Cai B (2016) Cancer cell membrane-coated upconversion nanoprobes for highly specific tumor imaging. Adv Mater 28:3460–3466

Rillings KW, Roberts JE (1974) A thermal study of the trifluoroacetates and pentafluoropropionates of praseodymium, samarium and erbium. Thermochim Acta 10:269–277

Russel C (1993) A pyrolytic route to fluoride glasses. Preparation and thermal decomposition of metal trifluoroacetates. J Non Cryst Solids 152:161–166

Schafer H, Ptacek P, Eickmeier H, Haase M (2009) Synthesis of hexagonal Yb^{3+}, E^{r3}+-doped NaY$_F$4 nanocrystals at low temperature. Adv Funct Mater 19:3091–3097

Scheps R (1996) Upconversion laser processes. Prog Quantum Electron 20:271–358

Schietinger S, Aichele T, Wang HQ (2010) Plasmon-enhanced upconversion in single NaYF$_4$: Yb^{3+}/Er^{3+} codoped nanocrystals. Nano Lett 10:134–138

Shao YZ, Liu LZ, Song S (2011) A novel one-step synthesis of Gd^{3+}-incorporated mesoporous SiO$_2$ nanoparticles for use as an efficient MRI contrast agent. Contrast Media Mol Imaging 6:110–118

Shikha S, Zheng X, Zhang Y (2017) Upconversion nanoparticles-encoded hydrogel microbeads-based multiplexed protein detection. Nano-Micro Lett 10:31

Sivakumar S, van Veggel FCJM, Raudsepp M (2005) Bright White light through up-Conversion of a single NIR source from sol−gel-derived thin film made with Ln^{3+}-Doped LaF$_3$ Nanoparticles. J Am Chem Soc 127:12464–12465

Son A, Dhirapong A, Dosev DK (2008) Rapid and quantitative DNA analysis of genetic mutations for polycystic kidney disease (PKD) using magnetic/luminescent nanoparticles. Anal Bioanal Chem 390:1829–1835

Sun Y, Chen Y, Tian L (2007) Controlled synthesis and morphology dependent upconversion luminescence of NaYF4: Yb Er nanocrystals. Nanotechnology 18:275609

Sun Y, Liu H, Wang X (2006) Optical spectroscopy and visible upconversion studies of YVO$_4$: Er^{3+} nanocrystals synthesized by a hydrothermal process. Chem Mater 18:2726–2732

Suyver JF, Aebischer A, Biner D (2005a) Novel materials doped with trivalent lanthanides and transition metal ions showing near-infrared to visible photon upconversion. Opt Mater (Amst) 27:1111–1130

Suyver JF, Grimm J, Kramer KW, Gudel HU (2005b) Highly efficient near-infrared to visible up-conversion process in NaYF$_4$: Er^{3+}, Y^{b3}+. J Lumin 114:53–59

Suyver JF, Grimm J, van Veen MK (2006) Upconversion spectroscopy and properties of NaYF$_4$ doped with Er^{3+}, Tm^{3+} and/or Yb^{3+}. J Lumin 117:1–12

Tsang MK, Ye W, Wang G (2016) Ultrasensitive detection of Ebola Virus oligonucleotide based on Upconversion nanoprobe/nanoporous membrane system. ACS Nano 10:598–605

van de Rijke F, Zijlmans H, Li S (2001) Up-converting phosphor reporters for nucleic acid microarrays. Nat Biotechnol 19:273–276

Vetrone F, Capobianco JA (2008) Lanthanide-doped fluoride nanoparticles: luminescence, upconversion, and biological applications. Int J Nanotechnol 5:1306–1339

Wang C, Cheng L, Xu H, Liu Z (2012) Towards whole-body imaging at the single cell level using ultra-sensitive stem cell labeling with oligo-arginine modified upconversion nanoparticles. Biomaterials 33:4872–4881

Wang F, Banerjee D, Liu Y (2010) Upconversion nanoparticles in biological labeling, imaging, and therapy. Analyst 135:1839–1854

Wang F, Deng R, Wang J (2011) Tuning upconversion through energy migration in core–shell nanoparticles. Nat Mater 10:968–973

Wang F, Han Y, Lim CS (2010) Simultaneous phase and size control of Upconversion nanocrystals through lanthanide doping. Nature 463:1061–1065

Wang F, Liu X (2008) Upconversion multicolor fine-tuning: visible to near-infrared emission from lanthanide-doped NaYF$_4$ Nanoparticles. J Am Chem Soc 130:5642–5643

Wang F, Liu X (2009) Recent advances in the chemistry of lanthanide-doped upconversion nanocrystals. Chem Soc Rev 38:976–989

Wang HQ, Nann T (2009) Monodisperse upconverting nanocrystals by microwave-assisted synthesis. ACS Nano 3:3804–3808

Wang L, Li P, Wang L (2009) Luminescent and hydrophilic LaF$_3$–polymer nanocomposite for DNA detection. Luminescence 24:39–44

Wang L, Li Y (2007) Controlled synthesis and luminescence of lanthanide doped NaYF$_4$ nanocrystals. Chem Mater 19:727–734

Wang L, Yan R, Huo Z (2005a) Fluorescence resonant energy transfer biosensor based on Upconversion-luminescent nanoparticles. Angew Chemie Int Ed 44:6054–6057

Wang X, Zhuang J, Peng Q, Li Y (2005b) A general strategy for nanocrystal synthesis. Nature 437:121–124

Wei Y, Lu F, Zhang X, Chen D (2006) Synthesis of oil-dispersible hexagonal-phase and hexagonal-Shaped NaYF$_4$:Yb, Er nanoplates. Chem Mater 18:5733–5737

Wisser MD, Chea M, Lin Y (2015) Strain-induced modification of optical selection rules in Lanthanide-Based Upconverting nanoparticles. Nano Lett 15:1891–1897

Xie X, Gao N, Deng R (2013) Mechanistic investigation of photon upconversion in Nd^{3+}-sensitized core–shell nanoparticles. J Am Chem Soc 135:12608–12611

Xie X, Liu X (2012) Upconversion goes broadband. Nat Mater 11:842–843

Xing H, Bu W, Zhang S (2012) Multifunctional nanoprobes for upconversion fluorescence, MR and CT trimodal imaging. Biomaterials 33:1079–1089

Xu H, Cheng L, Wang C (2011) Polymer encapsulated upconversion nanoparticle/iron oxide nanocomposites for multimodal imaging and magnetic targeted drug delivery. Biomaterials 32:9364–9373

Xu X, Wang Z, Lei P (2015) α-NaYb(Mn)F$_4$: Er^{3+}/Tm^{3+}@NaYF$_4$ UCNPs as "Band-Shape" luminescent nanothermometers over a wide temperature range. ACS Appl Mater Interfaces 7:20813–20819

Yang D, Dai Y, Liu J (2014) Ultra-small BaGdF$_5$-based upconversion nanoparticles as drug carriers and multimodal imaging probes. Biomaterials 35:2011–2023

Yang J, Li C, Cheng Z (2007) Size-tailored synthesis and luminescent properties of one-dimensional Gd_2O_3:Eu^{3+} nanorods and microrods. J Phys Chem C 111:18148–18154

Ye X, Collins JE, Kang Y (2010) Morphologically controlled synthesis of colloidal upconversion nanophosphors and their shape-directed self-assembly. Proc Natl Acad Sci 107: 22430–22435

Yi G, Lu H, Zhao S (2004) Synthesis, characterization, and biological application of size-controlled nanocrystalline $NaYF_4$: Yb, Er infrared-to-visible up-conversion phosphors. Nano Lett 4:2191–2196

Yi GS, Chow GM (2006) Synthesis of Hexagonal-Phase $NaYF_4$: Yb, Er and $NaYF_4$: Yb, Tm nanocrystals with efficient up-conversion fluorescence. Adv Funct Mater 16:2324–2329

Yi GS, Chow GM (2007) Water-soluble $NaYF_4$: Yb, Er(Tm)/NaY_F4/polymer core/shell/shell nanoparticles with significant enhancement of upconversion fluorescence. Chem Mater 19:341–343

Zeng JH, Su J, Li ZH (2005) Synthesis and upconversion luminescence of hexagonal-phase $NaYF_4$: Yb, Er^{3+} phosphors of controlled size and morphology. Adv Mater 17:2119–2123

Zhan Q, Liu H, Wang B (2017) Achieving high-efficiency emission depletion nanoscopy by employing cross relaxation in upconversion nanoparticles. Nat Commun 8:1058

Zhan Q, Qian J, Liang H (2011) Using 915 nm Laser Excited Tm^{3+}/Er^{3+}/Ho^{3+}-doped $NaYbF_4$ upconversion nanoparticles for in vitro and deeper in vivo bioimaging without overheating irradiation. ACS Nano 5:3744–3757

Zhang C, Chen J (2010) Facile EG/ionic liquid interfacial synthesis of uniform RE^{3+} doped $NaYF_4$ nanocubes. Chem Commun 46:592–594

Zhang H, Li Y, Ivanov IA (2010) Plasmonic modulation of the upconversion fluorescence in NaYF4:Yb/Tm hexaplate nanocrystals using gold nanoparticles or nanoshells. Angew Chemie Int Ed 49:2865–2868

Zhao J, Sun Y, Kong X (2008) Controlled synthesis, formation mechanism, and great enhancement of red upconversion luminescence of $NaYF_4$: Yb^{3+}, Er^{3+} nanocrystals/submicroplates at low doping level. J Phys Chem B 112:15666–15672

Zhu X, Zhou J, Chen M (2012) Core–shell Fe_3O_4@$NaLuF_4$: Yb, Er/Tm nanostructure for MRI, CT and upconversion luminescence tri-modality imaging. Biomaterials 33:4618–4627

Zhu YJ, Wang WW, Qi RJ, Hu XL (2004) Microwave-assisted synthesis of single-crystalline Tellurium nanorods and nanowires in ionic liquids. Angew Chemie Int Ed 43:1410–1414

Zou W, Visser C, Maduro JA (2012) Broadband dye-sensitized upconversion of near-infrared light. Nat Photonics 6:560–564